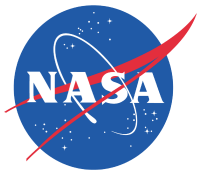

Planet Reliability Metrics: Astrophysical Positional Probabilities for Data Release 25

KSCI-19108-001

Stephen T. Bryson and Timothy D. Morton

February 28, 2017

NASA Ames Research Center
Moffett Field, CA 94035

Prepared by: _____ Date: February 28, 2017
Stephen T. Bryson, Kepler Science Office

Approved by: _____ Date: February 28, 2017
Michael R. Haas, Kepler Science Office Director

Approved by: _____ Date: February 28, 2017
Natalie Batalha, Kepler Project Scientist

Document Control

Ownership
This document is part of the Kepler Project Documentation that is controlled by the Kepler Project Office, NASA/Ames Research Center, Moffett Field, California.

Control Level
This document will be controlled under KPO @ Ames Configuration Management system. Changes to this document **shall** be controlled.

Physical Location
The physical location of this document will be in the KPO @ Ames Data Center.

Distribution Requests
To be placed on the distribution list for additional revisions of this document, please address your request to the Kepler Science Office:

Michael R. Haas
Kepler Science Office Director
MS 244-30
NASA Ames Research Center
Moffett Field, CA 94035-1000
Michael.R.Haas@nasa.gov

The correct citation for this document is: S. T. Bryson and T. Morton, 2017, *Planet Reliability Metrics: Astrophysical Positional Probabilities for Data Release 25,* KSCI-19108-001

Preface

This document is very similar to KSCI-19092-003, Planet Reliability Metrics: Astrophysical Positional Probabilities, which describes the previous release of the astrophysical positional probabilities for Data Release 24. The important changes for Data Release 25 are:

- The computation of the astrophysical positional probabilities uses the Data Release 25 processed pixel data for all Kepler Objects of Interest.
- Computed probabilities now have associated uncertainties, whose computation is described in §4.1.3.
- The scene modeling described in §4.1.2 uses background stars detected via ground-based high-resolution imaging, described in §5.1, that are not in the Kepler Input Catalog or UKIRT catalog. These newly detected stars are presented in Appendix B.

Otherwise the text describing the algorithms and examples is largely unchanged from KSCI-19092-003.

Revision History:

Date	Revision	Revision Description	Page(s)
2/28/17	KSCI-19108-001	Initial Release	

Contents

1 Introduction

This document describes the *Kepler* astrophysical positional probabilities (APP) table for Data Release 25 (DR25) hosted at the Exoplanet Archive[1]. This table lists the stars with the highest probability of being co-located with the source of an observed transit, as well as the probability of the transit being on an unknown background source. The position of the transit signal source relative to the target star is found in the KOI tables at the Exoplanet Archive. The probabilities provided in the APP table measure how likely it is that a star's location matches the location of the transit signal – they do not measure the probability that the transit signal is consistent with a planet orbiting that star.

For each star known to be near a *Kepler* Object of Interest (KOI), we compute the relative probability that the star is co-located with the transit source on the sky. We also compute the probability that the transit source is due to an unknown background source, relative to the probability for the known stars. These probabilities are relative in the sense that if one star has twice the probability of another, then the first star is twice as likely to be co-located with the transit source. Or if the probability for a star is twice the probability of the background, then that star is twice as likely to be the source of the transit as an unknown background source.

For a particular KOI, the relative probability is computed for stars that fall on the pixels associated with that KOI. These stars are provided by the catalogs described in §5. The APP table reports those probabilities for the KOI host, for the two stars with the highest probability, one of which may be the host star, and the background probability. Each of these probabilities is given an uncertainty, whose computation is described in §4.1.3.

Example uses of the APP relative probabilities include:

- Automatic identification of which background star is the source of the transit signal.
- Identification of spurious offsets by modeling bias in the offset measurements.
- Assessing the probability that the transit is a false positive when there is a background star very close to the KOI host star.

The first two use cases are discussed futher in §5.4. The relative probability that the transit signal source is co-located with the KOI host star is also of interest for exoplanet statistical studies. Derived planet properties depend critically on the details of the star that the planet orbits, and the planet properties reported in the *Kepler* planet candidate tables assume that the planet orbits the KOI host. So the probability that the transit signal is co-located with the host star, given in the APP table, provides a measure of the reliability that the derived planet properties are correct.

The reliability of the relative probabilities varies from KOI to KOI, and some KOIs will not have computed probabilities. These probabilities are computed using the results of centroid analysis of *Kepler* data as described in §4.1.1. The quality of the computed probabilities depends on the quality of the centroid data, and when the data is of low quality, for example

[1] http://exoplanetarchive.ipac.caltech.edu

when the transit S/N is very low, the resulting probabilities may be unreliable. The APP table provides a metric measuring the quality of the host star probability computation, which can be used to exclude unreliable probability computations. For many KOIs these centroids are unavailable or are known to be invalid, such as when the KOI host star is saturated or highly crowded. When the centroids are unavailable or invalid the probabilities are not computed, and the probability computation is declared to have failed.

The ability of the relative probabilities to distinguish between two known stars is determined by the accuracy of the underlying centroid data, which is in turn driven by the transit S/N. In some cases a star will have a relative probability near one while another star 1 arcsec away will have a probability near zero. In other cases, where the centroid measurements have lower spatial precision, the stars must be several arcsec apart to have different probabilities. The smallest distance that can be distinguished is 0.2 arcsec due to an observed centroid noise floor (see §4.1.3).

A simple alternative *a priori* probability of the transit signal being co-located with the target star is provided in the APP table for use in computing statistics when the probability computation is of low quality or has failed completely. This *a priori* probability is simply the fraction of KOIs whose transit signals are known to be offset from the KOI host star, which is a strong function of Galactic latitude (see §5.3). This *a priori* probability should be used statistically, and should not be applied to the analysis of individual KOIs.

When the relative probability computation fails only the fields Kepler ID, KOI name and *a priori* probability are set.

The APP table has the following structure. Archive variable names are given in parentheses.

- **Identification parameters:**
  - *Kepler* **ID** (*kepid*) of the KOI host star.
  - **KOI name** (*kepoi_name*) of the transit signal being analyzed.
  - **Period** (*pp_koi_period*) used in computing the relative probabilities. Not set when the probability computation fails.
  - **Epoch** (*pp_koi_time0bk*) used in computing the relative probabilities. Not set when the probability computation fails.
  - **Transit depth** (*pp_koi_depth*) in ppm used in computing the relative probabilities. Not set when the probability computation fails.
- **Host star probabilities:**
  - **Relative probability that the transit is co-located with the KOI host star** (*pp_host_rel_prob, pp_host_rel_prob_err*), or not set when the relative probability computation fails.
  - *A priori* **probability that the transit is co-located with the KOI host star** (*pp_host_prior_prob*), to be used when the relative probability computation fails. This is computed for all KOIs.

  - **Host star relative probability source flag** (*pp_host_prob_prov*). This flag takes one of the following values:
    * **PROB:** The relative probability score is computed using the method described in this document.
    * **MATCH:** The host star relative probability is set to zero because this KOI has been determined to be a period-epoch match and the parent is not among the known stars used in the relative probability computation (Coughlin et al., 2014).
    * **FPWG:** The relative probability computation failed but the host star relative probability is set to zero because the *Kepler* False Positive Working Group (FPWG) (Bryson et al., 2016) has examined this object and determined that the transit source is not co-located with the KOI host star. The state of this flag reflects false positive determinations by the FPWG prior to January 1, 2017.
    * **FAILED:** The relative probability computation failed and there is no alternative source of relative probabilities.
  - **Relative probability quality** (*pp_host_prob_score*). This quality value ranges from 0 to 1, and a value below about 0.3 indicates that the relative probability computation is likely to be untrustworthy.

- **The Two Highest Relative Probability Stars**: The two known stars with the highest probability of being co-located with the transit signal source. There may be only one known star considered in the probability computation. Several parameters are given for each star:
  - **Identifier of the star** (*pp_1hi_starid, pp_2hi_starid*). This may be a catalog number or a reference flag
  - **Star right ascension** (*pp_1hi_ra, pp_2hi_ra*) in degrees
  - **Star declination** (*pp_1hi_dec, pp_2hi_dec*) in degrees
  - **Star** *Kepler* **magnitude** (*pp_1hi_kepmag, pp_2hi_kepmag*). Depending on the source of information for this star, the *Kepler* magnitude uncertainty may be as large as two magnitudes.
  - **Relative probability that the transit is co-located with this star** (*pp_1hi_rel_prob, pp_1hi_rel_prob_err, pp_2hi_rel_prob, pp_2hi_rel_prob_err*).
  - **The modeled transit depth** (*pp_1hi_mod_depth, pp_2hi_mod_depth*) in parts per million that best reproduces the observed transit depth used in the relative probability computation described in §4.1.2. We do not expect this modeled depth to be accurate, but we provide it because it can indicate possible planetary-size transiting objects on stars other than the host star. This modeled depth depends critically on the accuracy of the catalog used to model the flux around the KOI host star and may be significantly in error. Therefore depths as large as 3 million

ppm are reported, so the modeled star may have to contribute negative flux in order to reproduce the observed depth. Stars whose modeled depths are greater than 3 million ppm are rejected from consideration by the relative probability computation. The probability computation is itself relatively insensitive to such large errors.

  - **Star provenance flag** (*pp_1hi_prob_prov, pp_2hi_prob_prov*) indicates the source of the position and magnitude information for this star.

- **Background Relative Probability** (*pp_unk_rel_prob, pp_unk_rel_prob_err*): The relative probability that the transit source is co-located with an unknown background object rather than a known star, described in §4.2.

- **Background Density** (*pp_bkgd_density*): The modeled density of background sources from Morton and Johnson (2011) used in the computation of the background relative probability.

The stars considered in the relative probability computation are from several sources. These sources are the Kepler Input Catalog (Brown et al., 2011), the UKIRT catalog (Lawrence et al., 2007) and various high-resolution imaging studies (see §5.1 and Appendix B). The source for a particular star is denoted by "KIC", "UKIRT" or "hires" in their ID, followed by the catalog identifier (The UKIRT catalog identifier is called "source ID" in the UKIRT catalog)[2].

Every KOI in the APP table that has a successful relative probability computation (Host star relative probability source flag = PROB) has an APP report giving a table of all stars that are considered in the relative probability computation. Each report also has a figure per star, showing its position relative to the target star and, when possible, contours showing the observed and modeled position distributions described in §4.1.3. These reports are available at the Exoplanet Archive.

The rest of this document describes the computation of the astrophysical position probabilities. §2 introduces and motivates the basic approach. In §3 we describe how probability is derived from likelihood via Bayesian hypothesis testing, and §4 describes the implementation. Specifically, §4.1.1 summarizes how transit locations are computed from the PRF-fit technique. §4.1.2 describes how transits are modeled on each known star. §4.1.3 derives the likelihoods from the modeled and observed data via smooth bootstrap techniques, with mathematical details given in appendix A. The likelihood of the transit source being an unknown background object is treated in §4.2. Results are given in §5, starting with a discussion of where the probability computation is unreliable. §5.4 illustrates the current method with a few examples.

[2]For instructions to access the UKIRT catalog, see http://keplergo.arc.nasa.gov/ToolsUKIRT.shtml.

2 A Probabilistic Approach to Background False Positive Identification

The *Kepler* Mission detects transiting exoplanets as well as background false positives that are observationally separated from the target star (Koch et al., 2010). The most common method for identifying background false positives is deriving the transit source location from various centroid techniques, and flagging a KOI as a false positive if its transit source location is more than 3σ from the target star (Bryson et al., 2013). Using the 3σ threshold makes it very unlikely that a transit signal on the target star will be misidentified as being on a background source. This 3σ threshold has been used to identify offset false positives in the KOI tables at the Exoplanet Archive (Burke et al., 2014; Mullally et al., 2015; Coughlin et al., 2016). This threshold is, however, somewhat crude and has the following weaknesses:

- Methods that measure centroids are subject to unknown systematic biases.
- When there are one or more known field stars within 3σ of the target star, applying the 3σ threshold does not account for any field stars that may be consistent with the data.
- The reliability of the claim that the transit signal is on the target star is interestingly different when the measured signal source position is, for example, 1σ vs. 2.8σ from the target star, but both cases pass the threshold.
- The rate of background binaries depends strongly on Galactic latitude (Bryson et al., 2013), but this is not reflected in the threshold.

Generally speaking, there is more information available about the location of a transit signal than a single position and a 3σ circle. This paper presents an analysis of the position of transit signals measured by *Kepler* using this additional information to compute the probability that the transit source is on a known star. These probabilities often provide more insight than the 3σ approach.

Several methods are used by the *Kepler* Mission to identify background false positives by determining that the observed position of the transit signal is not consistent with the target star position, as described in Bryson et al. (2013). In this paper we concentrate on the PRF-fit difference image technique (summarized in §4.1), which is the most robust and provides the highest precision. This method measures the position of a transit signal relative to the target star for each *Kepler* observational quarter by analyzing the pixel flux values for all transits in that quarter (see §4.1 for details). These measurements are subject to various systematic errors, in addition to photometric shot noise, which results in quarter-to-quarter variations of the measured centroid position. Averaging individual transits within a quarter is possible because *Kepler's* exceptional pointing stability means that each transit's flux variations stay on the same pixels. Across quarters, however, the stars fall on different pixels, preventing averaging at the pixel level.

The offset of the transit signal from the target star is estimated via an average of the quarterly offset measurements. Bryson et al. (2013) describes how this average is computed as a

χ^2 minimizing fit. This average, however, may not represent the true location of the transit source. Quarter-to-quarter systematics produce scatter in the quarterly position measurements, which can be thought of as a sampling of an unknown distribution of positions. The best estimate of the transit source location is given by the average of this unknown underlying distribution. The statistical bootstrap is an effective method of producing a *distribution of averages* of the measured quarterly transit location relative to the target star. The traditional bootstrap method provides the distribution of averages as a set of discrete points. We convert these points to a continuous distribution with the *smooth bootstrap* technique[3], which uses kernel density estimation techniques. We produce a continuous distribution of average *observed* positions $D_o(x, y)$ for the transit location and, via modeling of the transit on each star s, continuous *modeled* distributions $D_s(x, y)$. The models are based on stellar catalogs, observed transit parameters, the effective PSF of the Kepler instrument, and known noise sources as described in §4.1. We consider the degree of overlap of these distributions as a measure of the likelihood that a transit on star s is consistent with the observed transit location. We define the likelihood that the transit is on star s as the integral over the product of the distributions: $L_s = \int D_o(x, y)\, D_s(x, y)\, dx\ dy$. Because D_o and D_s are densities L_s has units of arcsecond^{-2}.

We compare the likelihood L_s that the transit is on star s with the likelihood L_t that the transit is on star t by computing the ratio $H_{st} = \frac{L_s}{L_t}$. All stars known to fall on the pixels collected for the target star are considered, as well as an unknown background. Similar to the treatment in Gregory (2010), we convert the hypothesis ratios H_{st} into probabilites in §3.

This modeling approach addresses the above described weaknesses of the 3σ threshold approach in several ways:

- Systematic crowding bias is accounted for, so long as that crowding is due to known stars.
- A continuous probability estimate more clearly describes borderline cases such as when there are stars within 3σ of the target star.
- The background binary density is accounted for so, for example, KOIs at low Galactic latitude are more likely to be due to background objects.

3 From Likelihood to Probability

Hypothesis testing considers the ratio $H_{st} = \frac{L_s}{L_t}$, where L_s was defined in §2. Hypothesis s is considered more likely than hypothesis t if $H_{st} > 1$.

The hypotheses ratios satisfy $H_{st} = H_{ts}^{-1}$, so there is a large amount of redundancy among the various H_{st}. In particular, thinking of H_{st} as a matrix for bookkeeping purposes, any

[3]See, for example, http://www.anawida.de/teach/SS12/compStat/Boots/smoothboot/smoothboot.pdf or Efron, B. and Tibshirani, R. J. (1994)

element can be expressed in terms of the elements of a specified column. For example, we can express any of the H_{st} in terms of the first column H_{s1}:

$$H_{st} = \frac{L_s}{L_t} = \frac{L_s}{L_1}\frac{L_1}{L_t} = H_{s1}H_{1t} = \frac{H_{s1}}{H_{t1}}.$$

We eliminate this redundancy and convert each column into a set of relative probabilities by normalizing each column by its sum: for each column t,

$$H_{st} \rightarrow \hat{H}_{st} \equiv \frac{H_{st}}{\sum_w H_{wt}} = \frac{L_s}{L_t}\frac{1}{\sum_w \frac{L_w}{L_t}} = \frac{L_s}{\sum_w L_w}. \quad (1)$$

These normalized hypothesis ratios $\hat{H}_{st}$ are independent of column: $\hat{H}_{st} = \hat{H}_{sw}$ for any t and w, and $\sum_s \hat{H}_{st} = 1$. So we can define the *probability of hypothesis s relative to the other hypotheses* as $R_s = \frac{L_s}{\sum_w L_w}$. R_s can be interpreted as a probability because $0 \leq R_s \leq 1$ and $\sum_s R_s = 1$.

4 Implementation

4.1 Modeling the Transit Signal on a Known Star

4.1.1 Measuring the Location of a Transit Source in the *Kepler* Pipeline

To set the context for how the transit signals are modeled and the resulting positions are measured, we briefly summarize how observed transit signal positions are measured relative to the target star. The *Kepler* Pipeline uses the *Kepler* Pixel Response Function (PRF), which provides a model of how the flux from a star falls on CCD pixels, given a star's position and magnitude. The transit source location is measured using the PRF-fit difference image method, which we describe briefly in the next paragraph. For details see Bryson et al. (2013).

An observed transit signal associated with a target star is identified and characterized from the flux light curve obtained by summing the pixels in an optimal photometric aperture around that target star (Jenkins et al., 2010, 2017). This photometric aperture is a subset of a larger pixel mask collected for each target star (Bryson et al., 2010b). For each quarter that contains transits, the in-transit cadences are identified. All pixels associated with this target star are then averaged over the in-transit cadences, creating the average *in-transit image*. Cadences on either side of each transit in a quarter are similarly used to create an average *out-of-transit image*. Subtracting the in-transit image from the out-of-transit image creates the *difference image* for each quarter. Assuming that the transit signal is the only source of flux variation between the in- and out-of-transit images, the difference image provides a direct image of the transit source. The location of that transit source is measured by fitting a PRF model to the difference image, which determines the star position for which the PRF-modeled flux distribution best matches the difference image pixel values. Though this PRF fit provides a formal propagated uncertainty based on the input pixel value uncertainties, it does not include the systematics described below.

The quarterly offset of the transit source from the target star is obtained by subtracting the position of the target star from the position of the transit source obtained from the PRF-fit to the difference image. The uncertainty of this offset is computed via standard propagation of errors. The position of the target star is obtained from a PRF fit to the out-of-transit image. Using the PRF fit of the out-of-transit image to measure the target star position is preferred over the input catalog target star position because systematic PRF fit errors due to inaccuracies in the PRF model are generally common to both the difference image and out-of-transit fits, and will often cancel out. In addition, the target star position in the input catalog has several sources of inaccuracy, such as unaccounted for proper motion. Using the PRF fit to the out-of-transit image assumes, however, that the target star is well-isolated so that this fit position gives the actual position of the target star. Crowding due to background stars will introduce a bias into the out-of-transit PRF fit position that is typically not present in the difference image. This introduces a crowding bias into the measurement of the transit source offset relative to the target star. One of the motivations for the work in this paper is to estimate this crowding bias for each target star. In extreme cases when there is another star of comparable or greater brightness near the target star, the PRF fit will typically return an incorrect target star position. For example, the PRF fit may return a value between the target star and that bright, nearby star, or may lock on to the position of the nearby star. If the out-of-transit PRF fit gives a target star location that is more than two arc seconds from the target star's catalog location, then the transit location offsets are considered invalid and the APP computation will be marked as "FAILED".

The PRF fit to the difference image is subject to various other systematics (Van Cleve et al., 2016), particularly due to flux variations other than the transit source, which introduce noise into the difference image. The result is that the quarterly offsets of the transit signal location relative to the target star will have some scattered distribution. While this scatter is statistically near-Gaussian (in particular it is zero-mean) when averaged over all targets, it may be far from Gaussian for specific target stars.

4.1.2 Modeling Transit Sources

For each target star, in each quarter in which transits occur, we create a synthetic out-of-transit image for the pixels in that target star's pixel mask using techniques similar to those described in Bryson et al. (2010b). Specifically, stellar catalogs and the *Kepler* PRF model (Bryson et al., 2010a) are used to add the flux from each star that is in or near the mask to the pixels in the synthetic image, scaled by that star's catalog flux. A star that is not in the mask is included if it is near enough to contribute flux to pixels in the mask according to the PRF model. The specific catalog used depends on the star and is identified in each target star's APP report.

The flux uncertainty σ_i^{OOT} of each out-of-transit pixel i is taken to be the observed uncertainty σ_i^{obs} computed by the *Kepler* pipeline (Jenkins et al., 2017). To compute the uncertainty of the difference image pixels, we estimate the non-photometric component of the σ_i^{OOT} by subtracting in quadrature the out-of-transit image's photometric uncertainty

$\sigma_i^{\rm phot,OOT}$ from the observed pixel uncertainty $\sigma_i^{\rm obs}$: $\sigma_i^{\rm pix} = \sqrt{\left(\sigma_i^{\rm obs}\right)^2 - \left(\sigma_i^{\rm phot,OOT}\right)^2}$. Here $\sigma_i^{\rm phot,OOT} = \sqrt{f_i^{\rm OOT}}/\sqrt{N}$ is the Poisson photon noise for each pixel with flux f_i, scaled by the square root of the number of out-of-transit cadences N.

For each star s in the target star's pixel mask, an in-transit image is created by the same method as for the out-of-transit image, but with the flux of star s scaled by $(1 - d_s)$ where d_s is the fractional depth of the simulated transit/eclipse if it were to occur on that star. The simulated depth d_s for each quarter is set by finding the value of d_s that best reproduces the observed depth $d^{\rm obs}$ in that quarter. First, the depth fit is seeded with the simple dilution-based estimate $d^{\rm obs}$ $f_{\rm target}/\sum_s f_s$ where $f_{\rm target}$ is the flux of the target star and f_s is the flux of star s (the target star is included in the sum over s). When the seed estimate of d_s is less than one, the d_s that matches $d^{\rm obs}$ is computed via a nonlinear Levenberg-Marquardt fit (Levenberg, 1944; Marquardt, 1963). This observed depth is not corrected for dilution by other flux in the aperture. When the seed estimate of d_s is greater than one, d_s is set equal to the seed value. This simulated depth is strongly dependent on the accuracy of the *Kepler* magnitudes of the stars used to model the flux on the pixels and can be inaccurate. We conservatively allow the depth to be as great as 3 (implying a reduction in the flux of the star by 300%). Stars whose modeled depth is greater than 3 are not considered in the probability computation and should be considered to have probability zero. We do not simulate transits on stars outside the pixel mask because centroid measurements for such stars are unreliable and can be very misleading.

The uncertainty of the modeled difference image pixels is estimated as $\sqrt{\left(\sigma_i^{\rm OOT}\right)^2 + \left(\sigma_i^{\rm IT}\right)^2}$, where $\sigma_i^{\rm IT} = \sqrt{\left(\sigma_i^{\rm phot,IT}\right)^2 + \left(\sigma_i^{\rm pix}\right)^2}$ is the estimated uncertainty of the in-transit image. Here $\sigma_i^{\rm phot,IT} = \sqrt{f_i^{\rm IT}}/\sqrt{N}$ is the Poisson photon noise for each in-transit image pixel with flux $f_i^{\rm IT}$, scaled by the square root of the number of out-of-transit cadences N, and $\sigma_i^{\rm pix}$ is that pixel's non-photometric noise estimated from the out-of-transit image as described above.

The result is that for each quarter we have a simulated average out-of-transit image and a collection of average in-transit images, with each difference image modeling the transit on a different known star in the target star's pixel mask. Each pixel of these average images has associated estimated uncertainties. The reader may ask why we did not build the simulated in-transit image from the observed out-of-transit image by injecting transit signals in the out-of-transit pixels. Simulated transits are placed on known stars at their catalog positions, and these catalog positions often disagree with the actual star positions due to, *e. g.*, catalog error and proper motion. Constructing the out-of- and in-transit images using the same catalog positions guarantees that the difference image is consistent with the out-of-transit image, eliminating the possibility of introducing biases in the modeling.

Similar to the observational data described in §4.1.1, a PRF fit is performed on the modeled out-of-transit image in each quarter q in which there is a transit, and, for each star s, on the modeled in-transit images. Taking the quarterly difference between the PRF fits of the in- and out-of-transit PRF fits gives us observed offsets $\Delta_{o,q} = \left(\Delta_{\rm RA}, \Delta_{\rm DEC}\right)_{o,q}$ with covariance matrix $\widetilde{\mathbf{\Sigma}}_o$, and modeled offsets $\Delta_{s,q} = \left(\Delta_{\rm RA}, \Delta_{\rm DEC}\right)_{s,q}$ with covariance matrix $\widetilde{\mathbf{\Sigma}}_s$

for each star s in the target star's pixel mask. In the next section we use these quarterly offsets to estimate distributions of the average observed and modeled offsets.

4.1.3 Computing the Likelihood for Each Star

The observed offsets of a transit signal location from the target star can be thought of as the sampling of an unknown distribution of offsets. The average of these observed offsets gives an estimate of the transit source location relative to the target star. If the transits were observed at a different time, we would get a different sampling of the unknown underlying distribution, with a different estimate of the transit source location. In this section we construct a distribution of these average offsets for both the observed and modeled transits. The overlap of the observed modeled distributions (see §5.4 for examples), defined as the integral of the product of the distributions, is the likelihood that the modeled star is the source of the transit.

For each collection of observed quarterly offsets $(\Delta_{\rm RA}, \Delta_{\rm DEC})_{o,q}$ and modeled quarterly offsets $(\Delta_{\rm RA}, \Delta_{\rm DEC})_{s,q}$ with their associated uncertainties, we construct a continuous distribution of mean average offsets using the *smooth bootstrap* technique. The smooth bootstrap starts with a conventional ensemble of bootstrap averages, and replaces each average value with a Gaussian distribution, similar to kernel density estimation (Silverman, 1986). Gaussian distributions are very convenient because products of Gaussians are Gaussians, and Gaussians lend themselves to explicit integration.

Given Q quarterly offsets $\Delta_{o,q}$ or $\Delta_{s,q}$, where Q is the number of quarters with a transit for the target, the bootstrap method generates an ensemble of N resampled offset sets, each of length Q, via resampling with replacement. The likelihood formula Eqn. 5 scales as N^2, which puts a practical limitation on the size of the bootstrap ensemble. We set $N = 500$ unless $Q < 5$, in which case we include every permutation of the data including repetitions (so $N = Q^Q$). Because $Q \leq 17$ this usually provides a sufficient sampling for the bootstrap estimate. However, as described below, we perform the likelihood computation 20 times with different bootstrap ensembles, providing a measure of the dependence of the probability computation on the bootstrap ensemble. The set of averages $\mathbf{b}_k$, $k = 1 \ldots N$, of each resampled set returned by the bootstrap method provides N average offsets. Each $\mathbf{b}_k$ is a two-dimensional vector with components giving the average RA and Dec offsets for each resampling. We denote the ensemble based on the observed offsets as $\mathbf{b}_{o,k}$ and those based on the modeled offsets for each star s as $\mathbf{b}_{s,k}$.

We smooth the bootstrap ensemble using a normalized two-dimensional Gaussian for each bootstrap average $\mathbf{b}_k$

$$G\left(\mathbf{x}, \mathbf{b}_k, \mathbf{\Sigma}\right) = \frac{1}{\sqrt{\det\left(2\pi\mathbf{\Sigma}\right)}} \exp\left[-\frac{1}{2}\left(\mathbf{x} - \mathbf{b}_k\right)^T \mathbf{\Sigma}^{-1}\left(\mathbf{x} - \mathbf{b}_k\right)\right] \tag{2}$$

where $\mathbf{x}$ and $\mathbf{b}_k$ are two-dimensional vectors (RA and Dec offsets in our case), and $\mathbf{\Sigma}$ is the covariance matrix that determines the smoothing, based on the covariance matrix of the original offsets $\widetilde{\mathbf{\Sigma}}_o$ or $\widetilde{\mathbf{\Sigma}}_s$ depending on whether we are smoothing the observed or modeled

distribution. We choose a two-dimensional generalization of Scott's rule-of-thumb (Scott, 1992):

$$\mathbf{\Sigma}_o = N^{-\frac{2}{d+4}} \widetilde{\mathbf{\Sigma}}_o, \qquad \mathbf{\Sigma}_s = N^{-\frac{2}{d+4}} \widetilde{\mathbf{\Sigma}}_s \tag{3}$$

where N is the number of averages in the bootstrap ensemble $\mathbf{b}_k$ and, in our case, $d = 2$. To account for an observed small residual bias in centroid offsets described in Bryson et al. (2013), a noise floor term of $(0.2/3 \text{ arcsec})^2$ is added to the diagonal terms of $\mathbf{\Sigma}_o$ and $\mathbf{\Sigma}_s$. This imposes a minimum size on the bootstrap distributions.

We define our smooth bootstrap distributions of the observed and modeled average offsets as

$$D_o(\mathbf{x}) = \frac{1}{N} \sum_{k=1}^{N} G(\mathbf{x}, \mathbf{b}_{o,k}, \mathbf{\Sigma}_o), \qquad D_s(\mathbf{x}) = \frac{1}{N} \sum_{k=1}^{N} G(\mathbf{x}, \mathbf{b}_{s,k}, \mathbf{\Sigma}_s). \tag{4}$$

With this definition $\int D_o(\mathbf{x})\, d\mathbf{x} = \int D_s(\mathbf{x})\, d\mathbf{x} = 1$, where $d\mathbf{x}$ is the two-dimensional RA and Dec area element.

We show in appendix A that our desired likelihood for the star s based on the smooth bootstrap technique is given by

$$L_s = \int D_o(\mathbf{x})\, D_s(\mathbf{x})\, d\mathbf{x} = \frac{1}{N^2} \sum_{k=1}^{N} \sum_{j=1}^{N} G(\mathbf{b}_{o,j}, \mathbf{b}_{s,k}, \mathbf{\Sigma}_o + \mathbf{\Sigma}_s) \tag{5}$$

This likelihood is computed 20 times using different randomly chosen bootstrap ensembles, and the final likelihood is computed as the average of these 20 trials, with the standard deviation providing an error estimate. We've found that using more than 20 trials does not provide significantly different results.

From these likelihoods we compute the probability that the star is in the same sky position as the transit source relative to other known stars as $R_s = \frac{L_s}{\sum_w L_w}$, where the sum includes the likelihood of the background described in the next section. The error in R_s is computed using standard propagation of errors. When $R_s < 10^{-30}$, we set $R_s = 0$ in the table.

4.2 The Background Likelihood

We model the hypothesis that the transit signal is due to an eclipse on an unknown background binary star using the background model of Morton and Johnson (2011). This model varies with target star *Kepler* magnitude and Galactic latitude. The *Kepler* magnitude dependence is due to this model's requirement that the background binaries produce a detectable transit-like signal when diluted by the target star. For a specific target star's pixel aperture this model is sufficiently slowly varying that we can take it as locally constant. We define b as the model background binary density per square arcsecond, evaluated for the target star.

To estimate b we use Equation (14) and Table 1 from Morton and Johnson (2011). We note that this table as published has the column values reversed: the absolute values of c_0 should be the largest and those of c_4 should be the smallest. For the targets modeled in this paper, b ranges from 1.6×10^{-6} to 5.1×10^{-5} background binaries per square arcsecond, with a median of 1.1×10^{-5}.

Given b, in order to satisfy the requirement that our distributions are normalized we define the background distribution as

$$D_{\rm bgd}\left(\mathbf{x}\right) = \begin{cases} b, & r \leq \frac{1}{\sqrt{\pi b}} \\ 0, & r > \frac{1}{\sqrt{\pi b}} \end{cases} \tag{6}$$

where $r = \sqrt{x^2 + y^2}$. So $D_{\rm bgd}\left(\mathbf{x}\right) = b$ in a circle of radius $R_0 = 1/\sqrt{\pi b}$, is zero outside this circle, and $\int D_{\rm bgd}\left(\mathbf{x}\right)\ dx\ dy = 1$. The smallest radius for this circle occurs when b is largest, where $R_0 = 79$ arcseconds or about 20 *Kepler* pixels. A 20 pixel radius is larger than the largest pixel mask for a non-saturated target star, so this normalization is appropriate for comparison with the normalized Gaussians we use to compute our likelihoods.

The background likelihood is $L_{\rm bgd} = \int D_{\rm bgd} D_o d\mathbf{x}$, and because b vanishes outside the circle of radius R_0, the product in the integrand vanishes as well. This is plausible because for any reasonable measurement of the centroid position, D_o should essentially vanish outside a circle that is considerably smaller than 79 arcseconds: the pixel mask for a 12th magnitude star typically has a radius of about 25 arcseconds. Therefore no information is lost by imposing a background model that vanishes outside a circle of radius ≥ 79 arcseconds. We demonstrate this by assuming that D_o is a Gaussian with a diagonal covariance matrix with equal entries, so D_o becomes a function of r only. Then the likelihood of the background hypothesis is

$$L_{\rm bgd} = \int D_{\rm bgd} D_o d\mathbf{x} = \int_0^\infty D_{\rm bgd} D_o\ dr = b \int_0^{R_0} D_o\ dr. \tag{7}$$

Now $\int_0^\infty D_o\ dr = 1$ and $\int_0^{R_0} D_o\ dr = \int_0^\infty D_o\ dr - \int_{R_0}^\infty D_o\ dr = 1 - \int_{R_0}^\infty D_o\ dr$, so

$$L_{\rm bgd} = b\left(1 - \int_{R_0}^\infty D_o\ dr\right). \tag{8}$$

If we make the conservative assumption that the uncertainty of D_o is 5 arcseconds (see Fig 33 of Bryson et al. (2013)), then $\int_{R_0}^\infty D_o\ dr \approx 10^{-110}$, which can be neglected. Because this example is computed based on the highest background density and largest reasonable measurement uncertainty, we can generally take $L_{\rm bgd} = b$. While this analysis made various simplifying assumptions, a more realistic analysis is not expected to significantly change the results. The error in the background probability is determined by the propagation of the error in the individual likelihoods described at the end of §4.1.3.

5 Results

The purpose of the methods described in this paper is to compute the relative probability that

- the transit signal source is likely to be in the same location as the target star
- the transit source is likely to be in the same location as a known star other than the target star

- the transit source is likely to be in the background population of unknown stars.

The relative probabilities described in this paper have been computed for identified KOIs (Thompson et al., 2017) that have the following properties:

- The *Kepler* magnitude is dimmer than 10, because PRF fitting breaks down for brighter targets, which are highly saturated.
- The PRF fit to the observed out-of-transit image, which measures the position of the target star (see §4.1.1), is within 2 arcsec of the catalog position of the target star. When this condition is violated, either there is sufficient crowding to invalidate the centroid data or the target star catalog position is incorrect, invalidating the modeling behind the relative probability computation.
- PRF-fit centroids were successfully computed by the *Kepler* pipeline. The PRF fitting process often fails for low S/N transit signals.

KOIs not satisfying these criteria are marked "FAILED" in the APP table and no relative probabilities are available.

5.1 Input Stellar Catalogs

For creation of the synthetic scene we use the *Kepler* Input Catalog (KIC) (Brown et al., 2011) (6,517,562 objects) supplemented by the UKIRT catalog (Lawrence et al., 2007) (5,972,148 objects) and an assortment of high-resolution imaging studies (873 objects). The UKIRT catalog was federated with the KIC by removing stars already in the KIC and estimating *Kepler* magnitudes from the UKIRT J magnitudes assuming all stars are on the main sequence. The errors on the UKIRT-based *Kepler* magnitudes can be as large as 2 magnitudes. Objects discovered by the high-resolution imaging studies are described and presented in Appendix B.

5.2 Host Star Relative Probability Quality

There are several ways in which the computed probabilities can be misleading. We concentrate on the two most common problem cases:

- Transits with S/N < 10 often do not have enough signal in each pixel of the difference image to produce a reliable PRF fit.
- Crowding by bright field stars can invalidate the probability analysis. Most of these cases are removed by marking KOIs whose PRF-fit target star positions are more than 2 arcsec from their catalog positions as "FAILED", but bias may remain in other cases.

We indicate the host star relative probability quality using *Relative Probability Quality*, a numerical score that measures the likelihood of these problems. This score ranges from 0 to 1, and we recommend trusting the probabilities reported for the target star when this score

is about 0.3 or above. Relative Probability Quality is the product of two metrics, each of which is normalized to range from 0 to 1:

- **Difference Image Quality** which measures how well the transit signal difference image resembles a star. In each quarter we compute the correlation of the fitted PRF model with the pixel data (Bryson et al., 2013). The difference image quality metric is the number of quarters where the correlation is > 0.7 divided by the total number of quarters in which a transit was observed.

- **Local Crowding** which compares the flux in the target star's optimal aperture with the flux outside the optimal aperture in the star's pixel mask. When the flux outside the optimal aperture exceeds that in the optimal aperture by about a factor of two, then the PRF fit to the out-of-transit image is considered unreliable. The local crowding metric uses the inverse of this ratio with a non-linear sigmoid function to produce a crowding score between 0 and 1, with 1 indicating that most of the flux is from the optimal aperture, and 0.5 indicating that about the same amount of flux is inside the optimal aperture as outside.

5.3 Host Star *a priori* Probability

When the host star relative probability quality score described in §5.2 is below threshold, there are several alternatives. When possible, the user should examine the transit data to make a determination of the quality of the centroid measurements using the concepts in Bryson et al. (2013). When this is not possible, such as when many targets are being analyzed for a statistical study, or when examination shows that there is essentially no information on the transit signal source location, we recommend using the *a priori* target star probability values supplied in the table. These are based on the observation that the probability of a *Kepler* object of interest being on the target star depends sensitively on Galactic Latitude (Bryson et al., 2013). Both the observed offset false positive fraction shown in Figure 1 and modeling (Morton and Johnson, 2011) indicate such a dependence on Galactic latitude. This fraction's dependence on Galactic latitude is relatively insensitive to target star and transit properties. The *a priori* target star probability is a fit to the fraction of KOIs that are on the target star to the total number of KOIs at a given Galactic latitude.

5.4 Examples

The confirmed planet Kepler-11c is shown in Figure 2. In this example the observed centroids are clustered around the KOI host star KIC 6541920, so the target star is near the center of the bootstrap distribution of observed averages, shown by the green contours. Modeling the transit on the target star produces a distribution of averages, shown by the magenta contours, that is also nearly centered on the target star. The overlap of the observed (green) and modeled (magenta) distributions leads to a large likelihood and a 100% probability that the transit signal is co-located with the target star.

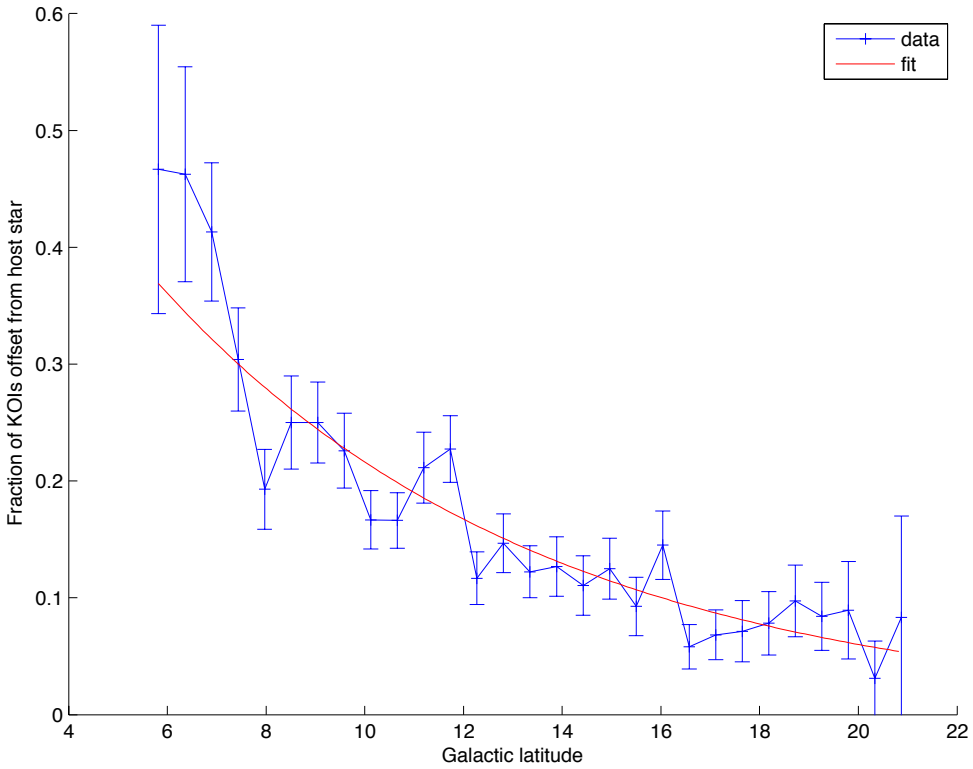

Figure 1: Blue: The fraction of KOIs that have been identified as background false positives via offsets from their KOI host stars as a function of Galactic Latitude. The error bars show the 1σ Poisson uncertainty. Red: the fit used to compute the KOI host star a priori probability. The fit is $y = 0.775 \times 10^{(-0.0556x)}$ where x is the Galactic latitude in degrees.

A background false positive, KOI 109.01, associated with a known background star is shown in Figure 3. In this case the green contours, showing the distribution of observed averages, are very near the background star KIC 4752452 and very far from the KOI host star KIC 4752451, indicating that the KOI host is unlikely to be the source of the transit signal. The KOI host star has a probability of zero, while there is a 98.9% relative probability that the transit source is at the location of KIC 4752452. Because the green observed contours have only a small overlap with the magenta contours obtained by modeling the transit on KIC 4752452, the background has a probability of 1.1%.

Figure 4 shows the interesting case of KOI-582.01, where an apparent offset in the centroids from the KOI host star turns out to be spurious, caused by centroid bias due to crowding by a bright star outside the figure. This bias is revealed by modeling the transit on the KOI host star KIC 9020160. The modeled magenta contours show that the expected distribution of averages is offset from KIC 9020160 in the same direction and distance as the green observed contours. Therefore the original disposition of KOI-582.01 as a false positive because its measured centroid offset is more than 3σ from the target star (shown by the cyan circle) is incorrect.

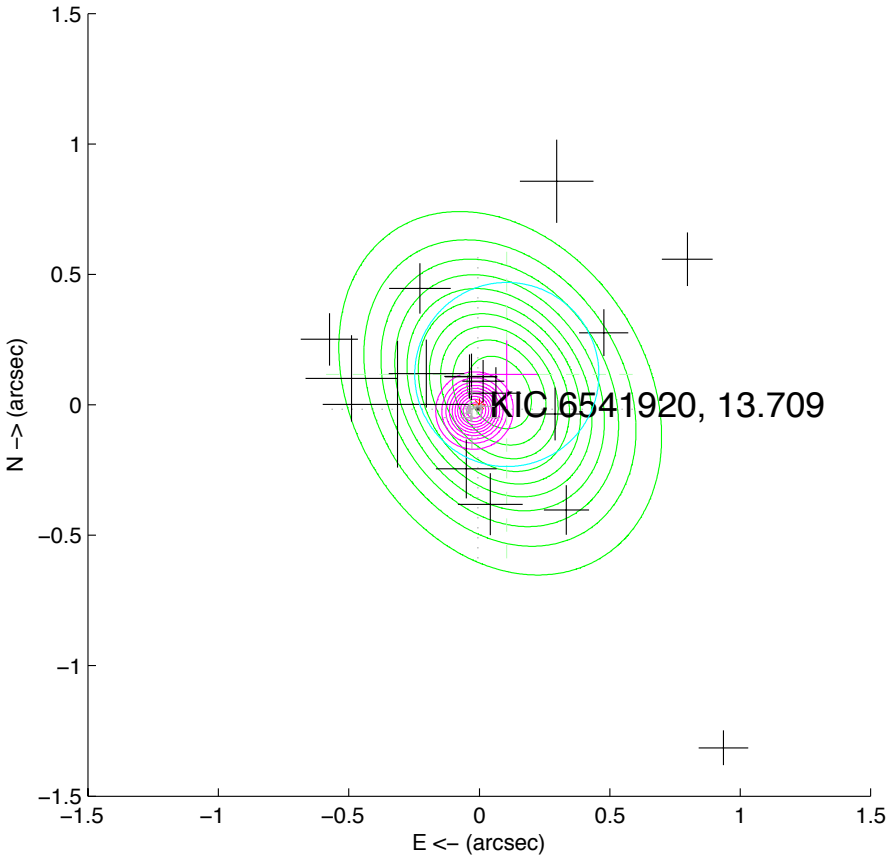

Figure 2: Results of the probability analysis for KOI-157.01 (confirmed planet Kepler-11c) with target star KIC 6541920, *Kepler* magnitude 13.709. In this example the transit signal location is strongly consistent with the target star. The distribution of averages of the observed transit positions D_o is rendered as green contours, while the magenta contours show the distribution D_{target} with the transit modeled on the target star. The target star is shown as a red asterisk, the black crosshairs are the observed quarterly transit locations, and the light grey dashed crosshairs are the modeled transit locations. In this example the modeled transit locations are very tightly clustered so the magenta contours are close to the target star. The magenta crosshair and cyan circle show the χ^2 average position and 3σ radius produced by the data validation module of the *Kepler* pipeline (Jenkins et al., 2017), used in conventional planet candidate vetting (Coughlin et al., 2016).

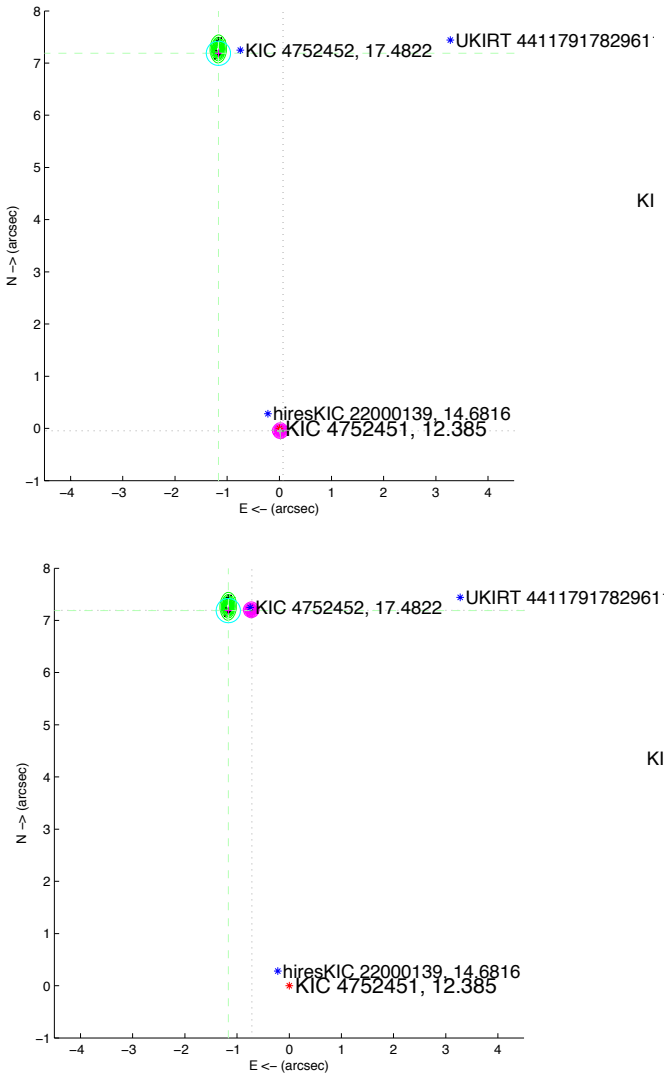

Figure 3: Results of the probability analysis for KOI-109.01 with target star KIC 4752451, *Kepler* magnitude 12.385. In this example the transit signal location is strongly inconsistent with the target star, and is consistent with the 17th magnitude field star KIC 4752452, shown by a blue asterisk. Top: the transit modeled on the target star KIC 4752451, so the modeled magenta contours and the observed green contours are very far apart. Bottom: the transit modeled on KIC 4752452, with the modeled magenta contours slightly overlapping with the green observed contours. Though the overlap is small, it is large enough for a 98.9% probability that the transit is co-located with KIC 4752452, while the background probability is 1.1%. See Figure 2 for a description of elements of the figure.

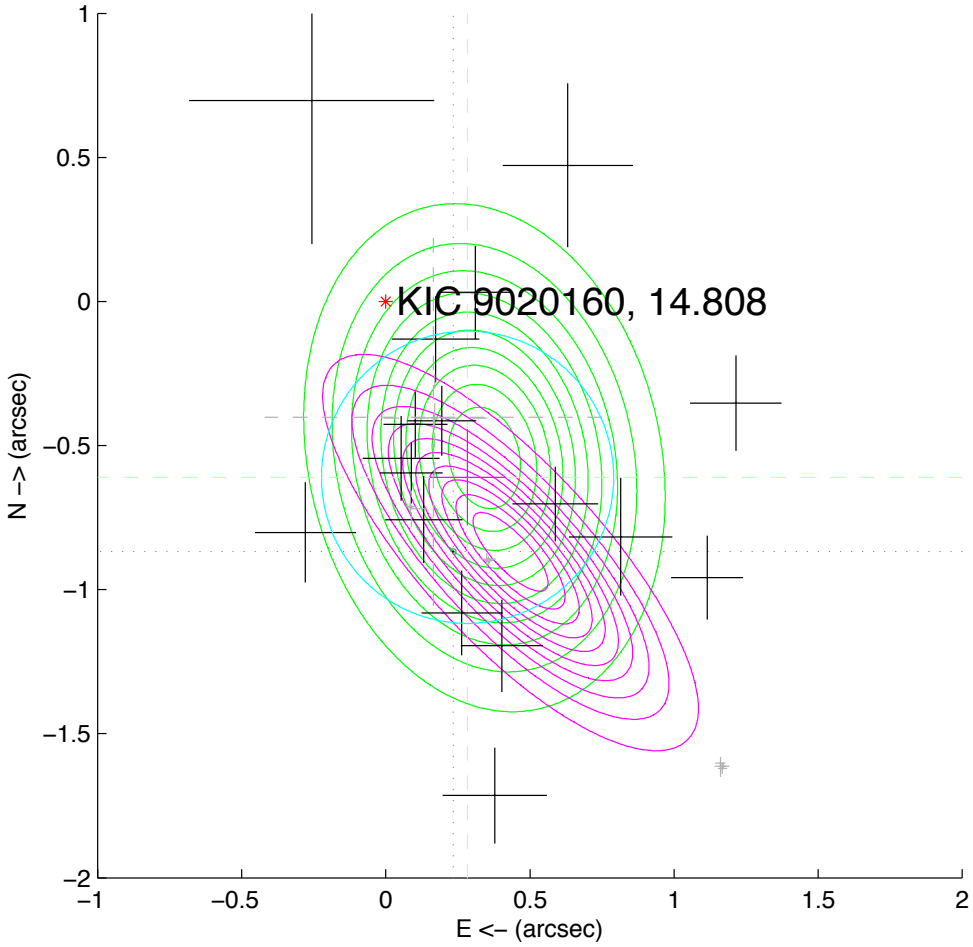

Figure 4: Results of the probability analysis for KOI-582.01 with target star KIC 9020160, *Kepler* magnitude 14.808. In this example the transit signal location is more than 3σ away from the target star, as indicated by the cyan circle offset to the SW. The conclusion that the transit source is offset from the target star is reinforced by the location of the black crosshairs showing the quarterly transit offsets. The observed distribution shown by the green contours is also offset, consistent with the 3σ circle. But the observed distribution is consistent with the modeled distribution shown by the magenta contours, which are offset from the target star due to crowding bias caused by a bright nearby star outside the figure. Therefore it would be incorrect to declare this KOI to be a background false positive. See Figure 2 for a description of elements of the figure.

Appendix A

We use the notation of §4.1.3. Our desired likelihood for each star s is the integral of the product

$$L_s = \int D_o\left(\mathbf{x}\right) D_s\left(\mathbf{x}\right) d\mathbf{x}. \tag{9}$$

The product of two Gaussians is the Gaussian

$$G\left(\mathbf{x}, \mathbf{b}_{o,j}, \mathbf{\Sigma}_o\right) G\left(\mathbf{x}, \mathbf{b}_{s,k}, \mathbf{\Sigma}_s\right) = c_{j,k} G\left(\mathbf{x}, \mathbf{m}_{j,k}, \mathbf{\Phi}\right) \tag{10}$$

where

$$\begin{aligned} c_{j,k} &= G\left(\mathbf{b}_{o,j}, \mathbf{b}_{s,k}, \mathbf{\Sigma}_o + \mathbf{\Sigma}_s\right) \\ \mathbf{m}_{j,k} &= \left(\mathbf{\Sigma}_o^{-1} + \mathbf{\Sigma}_s^{-1}\right)^{-1} \left(\mathbf{\Sigma}_o^{-1}\mathbf{b}_{o,j}, +\mathbf{\Sigma}_s^{-1}\mathbf{b}_{s,k}\right) \\ \Phi &= \left(\mathbf{\Sigma}_o^{-1} + \mathbf{\Sigma}_s^{-1}\right)^{-1}. \end{aligned} \tag{11}$$

so

$$\begin{aligned} L_s &= \int D_o\left(\mathbf{x}\right) D_s\left(\mathbf{x}\right) d\mathbf{x} \\ &= \frac{1}{N^2} \int \sum_{k=1}^{N} \sum_{j=1}^{N} G\left(\mathbf{x}, \mathbf{b}_{o,k}, \mathbf{\Sigma}_o\right) G\left(\mathbf{x}, \mathbf{b}_{s,j}, \mathbf{\Sigma}_s\right) d\mathbf{x} \\ &= \frac{1}{N^2} \int \sum_{k=1}^{N} \sum_{j=1}^{N} c_{j,k} G\left(\mathbf{x}, \mathbf{m}_{j,k}, \mathbf{\Phi}\right) d\mathbf{x} \\ &= \frac{1}{N^2} \sum_{k=1}^{N} \sum_{j=1}^{N} c_{j,k} \end{aligned} \tag{12}$$

because $\int G\left(\mathbf{x}, \mathbf{m}_{j,k}, \mathbf{\Phi}\right) d\mathbf{x} = 1$.

Appendix B

This appendix describes the detection of 873 objects via high-resolution imaging by Adams et al. (2012), Dressing et al. (2014), Wolfgang (2015), the Robo-AO program (Law et al., 2014; Baranec et al., 2016; Ziegler et al., 2016) and the *Kepler* follow-up observation program (Furlan et al., 2016). These sources used a variety of telescopes and observed in a variety of colors, so the federation of these results with the KIC/UKIRT and each other was challenging. In some cases the authors provided *Kepler* magnitude estimates. In other cases *Kepler* magnitudes were estimated using methods that depend on the available colors as described below.

Data about the 873 objects detected by high-resolution imaging are provided as position and magnitude offsets from the target star. Nearby "background" objects detected by high-resolution imaging may be bound companions of the target star in the KIC. In some cases, such as KOI-284, the KIC entry for the target star is resolved into two nearly equal-brightness stars, one of which is taken by the observer to be the target star. In such cases different observers sometimes make different choices for which imaged star is the target star, making the offsets reported by one observer inconsistent with the offsets reported by another. These cases are identified via manual inspection, and are resolved by rejecting one of the observer's data.

In several cases the same new star was identified by several observers, but with slightly different positions and magnitudes. Observations that cluster within 0.5 arcsec of each other and whose *Kepler* magnitude estimates are within 4 magnitudes of each other (due to the large *Kepler* magnitude uncertainties in some of the conversions from other bandpasses) are considered to be the same background object. Clusters containing a KIC or UKIRT star are identified with that KIC or UKIRT star and are removed. The position of each remaining cluster is defined as the average of the position estimates in that cluster. The *Kepler* magnitude of each remaining cluster is the flux average of the *Kepler* magnitude estimates in that cluster. The resulting cluster positions and *Kepler* magnitudes are used to define new background objects considered in addition to the KIC and UKIRT stars. The KIC and UKIRT catalogs were not modified.

The table below gives data for the 873 objects defined via this clustering algorithm.

- **ID** is the assigned number of the object. This number appears in the table and figures prepended with "hires".
- **Kp** is the *Kepler* magnitude for the object, defined as above.
- **hostID** is the KIC ID of the target star used as the reference for delta RA and delta Dec.
- **sep** is the separation in arcsec of this object from the target star identified by **hostID**.
- **ΔRA** is the delta RA in arcsec of this object from the target star identified by **hostID**.
- **ΔDec** is the delta Dec in arcsec of this object from the target star identified by **hostID**.

- **source** provides the source of the observational data for this object as a list of reference and magnitude codes for the observations defining this object. Each reference has its own magnitude codes.

  - **adams** (Adams et al., 2012), which provides estimated *Kepler* magnitude. The magnitude codes give the instrument used for the observation.
    - **_P** Was observed with the Aries instrument.
    - **_A** Was observed with the Pharo instrument.

  - **dressing** (Dressing et al., 2014), which provides estimated *Kepler* magnitude. Only one instrument and color was used so there are no magnitude codes.

  - **fop** (Furlan et al., 2016), which uses a variety of instruments and colors that vary from observation to observation. The *Kepler* magnitude estimate for a star depends on the available colors in which that star was observed. Some colors are preferred over others, so the following magnitude codes are listed in order of preference. The error in the estimated *Kepler* magnitude grows from ~ 0.03 magnitudes at the top to more than 2 magnitudes at the bottom of the list. If a code later in this list is used, this means the colors for earlier codes are not available.
    - **_gri:** Two or more of g, r, or i magnitudes are available. g magnitude is available when the target star has g magnitude in the KIC and (in order of preference) deltaVmag, deltaVF555W, or deltaBmag is provided, which is taken as delta g magnitude. r magnitude is available when the target star has r magnitude in the KIC and deltaVF775W is provided, which is taken as delta r magnitude. i magnitude is available when the target star has i magnitude in the KIC and deltaImag is provided. Then *Kepler* magnitude is estimated using Equation 2 of Brown et al. (2011).
    - **_692:** Delta692 is provided, which can be taken as delta *Kepler* magnitude and added to the target star's *Kepler* magnitude.
    - **_LP600:** DeltaLP600 is provided, which can be taken as delta *Kepler* magnitude and added to the target star's *Kepler* magnitude.
    - **_LP562:** DeltaLP562 is provided, which can be taken as delta *Kepler* magnitude and added to the target star's *Kepler* magnitude.
    - **_jhk:** Delta j, delta h and delta k are provided and the KIC supplies j, h and k magnitudes. Estimate the *Kepler* magnitude using the formulas in the Appendix of Howell et al. (2012) when these magnitudes are in the required ranges.
    - **_jk:** Delta j and delta k are provided and the KIC supplies j and k magnitudes. Estimate the *Kepler* magnitude using the formulas in the Appendix of Howell et al. (2012) when these magnitudes are in the required ranges.

    - **_j:** Delta j is provided and the KIC supplies j magnitude. Estimate the *Kepler* magnitude using the formulas in the Appendix of Howell et al. (2012).
    - **_k:** Delta k is provided and the KIC supplies k magnitude. Estimate the *Kepler* magnitude by interpolating a second-order polynomial fit of all KIC k magnitudes to *Kepler* magnitude.
    - **_h:** Delta h is provided and the KIC supplies h magnitude. Estimate the *Kepler* magnitude by interpolating a second-order polynomial fit of all KIC h magnitudes to *Kepler* magnitude.
    - **_i:** Delta i is provided and the KIC supplies i magnitude. Estimate the *Kepler* magnitude by interpolating a second-order polynomial fit of all KIC i magnitudes to *Kepler* magnitude.
    - **_deltaKp=DeltaV:** Delta v is provided but the KIC does not supply a v magnitude. Delta v is taken as delta *Kepler* magnitude and added to the target star's *Kepler* magnitude.
    - **_deltaKp=DeltaZ:** Delta z is provided but the KIC does not supply a z magnitude. Delta z is taken as delta *Kepler* magnitude and added to the target star's *Kepler* magnitude.
    - **_deltaKp=Delta880:** Delta880 is provided but the KIC does not supply a corresponding magnitude. Delta880 is taken as delta *Kepler* magnitude and added to the target star's *Kepler* magnitude.
    - **_deltaKp=DeltaJ:** Delta j is provided but the KIC does not supply a j magnitude. Delta j is taken as delta *Kepler* magnitude and added to the target star's *Kepler* magnitude.

- **roboAO** (Law et al., 2014; Baranec et al., 2016; Ziegler et al., 2016), which uses two colors: LP600 and i.
    - **_LP600:** deltaLP600 is provided, which can be taken as delta *Kepler* magnitude and added to the target star's *Kepler* magnitude.
    - **_i:** Delta i is provided and the KIC supplies i magnitude. The *Kepler* magnitude is estimated by interpolating a second-order polynomial fit of all KIC i magnitudes to *Kepler* magnitude.
    - **_deltaiEqDeltaKp:** Delta i is provided but the KIC does not supply an i magnitude. Delta i is taken as delta *Kepler* magnitude and added to the target star's *Kepler* magnitude.

- **wolfgang** (Wolfgang, 2015) provides estimated *Kepler* magnitude based on observations in one or more of j, h and/or k. The color codes indicate which of these colors was used for the *Kepler* magnitude estimate: **_jhk**, **_hk**, **_jk**, **_jh**, **_j**, **_h**, **_k**.

ID	Kp	hostID	sep	ΔRA	ΔDec	source
22000001	11.71	1161345	1.75	-1.18	-1.29	fop_gri wolfgang_jhk
22000002	18.68	1161345	4.80	2.81	-3.89	wolfgang_h
22000003	14.65	1429589	0.78	0.65	-0.42	roboAO_LP600
22000004	17.64	1575873	0.87	0.82	-0.27	fop_692
22000005	15.34	1865042	0.30	0.04	-0.29	fop_i roboAO_i wolfgang_k
22000006	15.90	2013883	2.15	-1.89	-1.02	fop_jk roboAO_LP600
22000007	21.07	2162635	1.08	0.46	-0.98	fop_k
22000008	20.95	2162635	1.21	0.66	1.01	fop_k
22000009	14.96	2167890	1.30	1.15	-0.60	fop_deltaKp=DeltaZ
22000010	16.75	2167890	1.90	1.89	-0.10	fop_deltaKp=DeltaZ
22000011	18.69	2302548	8.82	0.04	-8.82	wolfgang_h
22000012	13.47	2306756	0.17	0.04	-0.17	adams_P fop_692
22000013	20.66	2306756	3.16	-2.93	1.18	adams_P fop_jk
22000014	20.57	2306756	3.58	2.60	2.45	adams_P fop_j
22000015	21.15	2437149	1.77	0.52	-1.69	fop_j
22000016	20.41	2437452	3.78	0.17	-3.78	fop_j
22000017	18.89	2437783	3.39	-3.30	0.77	fop_j
22000018	18.62	2437783	3.44	0.87	-3.33	fop_j fop_j
22000019	19.63	2438062	1.27	1.04	-0.73	fop_j
22000020	21.13	2438406	1.79	-0.86	-1.57	fop_k
22000021	22.44	2441161	1.75	1.65	-0.56	fop_j
22000022	15.71	2446113	1.09	-0.91	0.60	fop_692
22000023	14.56	2446113	2.02	2.00	0.29	fop_gri roboAO_LP600
22000024	14.81	2449074	1.79	-1.22	1.32	fop_j
22000025	15.47	2449074	2.91	0.61	2.85	fop_j
22000026	20.50	2449090	2.44	2.43	-0.08	fop_j
22000027	17.84	2449431	1.51	0.11	-1.51	fop_LP600 roboAO_LP600 wolfgang_jhk
22000028	20.59	2558370	2.69	2.69	0.10	fop_deltaKp=DeltaJ
22000029	19.97	2569494	1.53	-1.04	1.13	fop_i
22000030	20.15	2569494	2.87	-2.79	0.64	fop_i
22000031	20.60	2584163	3.48	3.30	-1.12	fop_j
22000032	13.27	2696703	2.61	2.41	1.01	fop_k roboAO_LP600
22000033	23.30	2853029	1.36	-0.94	0.98	fop_gri
22000034	20.51	2853029	2.17	-1.18	1.81	fop_gri
22000035	12.28	2853828	0.94	-0.94	0.06	fop_jk roboAO_LP600
22000036	19.78	2856960	1.48	1.21	-0.85	fop_k
22000037	18.18	2859893	1.41	0.20	-1.40	roboAO_LP600
22000038	12.55	2985767	0.06	0.05	-0.04	fop_692
22000039	12.61	2985767	1.14	-0.77	0.84	fop_692 roboAO_LP600

ID	Kp	hostID	sep	ΔRA	ΔDec	source
22000040	13.55	3003992	0.47	0.43	0.20	fop_k
22000041	15.00	3097346	0.46	0.28	0.36	adams_A fop_jk
22000042	19.57	3098810	2.54	2.51	-0.38	fop_h
22000043	17.02	3101923	1.51	0.59	1.39	roboAO_LP600
22000044	18.50	3102384	5.51	1.66	5.25	adams_A
22000045	21.87	3114167	3.39	0.09	3.39	fop_j
22000046	20.64	3117115	3.76	-3.53	1.29	fop_j
22000047	18.85	3120904	2.45	-0.21	2.44	roboAO_LP600
22000048	20.75	3228804	3.83	3.28	-1.98	fop_j
22000049	9.83	3230227	1.75	-1.64	0.60	roboAO_LP600
22000050	20.48	3232859	3.72	-2.33	2.90	fop_j
22000051	17.18	3234598	0.31	0.29	0.12	fop_LP600 roboAO_LP600
22000052	19.01	3239945	2.16	1.92	0.98	fop_j
22000053	18.06	3245969	1.71	-0.62	1.59	fop_k
22000054	19.95	3247396	2.85	0.58	-2.79	adams_P fop_j
22000055	20.07	3247396	3.67	-0.57	-3.62	adams_P fop_j
22000056	16.25	3326377	0.46	-0.30	0.34	fop_jk roboAO_LP600
22000057	19.10	3341982	1.23	-1.09	-0.58	roboAO_LP600
22000058	15.45	3346543	1.22	-1.20	0.19	roboAO_LP600
22000059	13.91	3425851	1.79	-1.78	-0.12	fop_LP600 roboAO_LP600 wolfgang_
22000060	18.82	3425851	9.77	-9.70	1.20	wolfgang_jk
22000061	13.14	3433668	0.74	0.74	0.01	roboAO_LP600
22000062	14.14	3438975	0.16	-0.11	0.12	fop_692
22000063	10.20	3441784	0.25	0.19	-0.17	fop_692 roboAO_deltaiEqDeltaKp
22000064	15.21	3446746	2.10	-1.93	-0.83	fop_i
22000065	13.39	3458919	2.02	-1.91	-0.68	fop_j
22000066	17.00	3531558	1.27	-0.71	-1.06	adams_P fop_692
22000067	16.88	3534076	0.50	0.10	-0.48	fop_jk
22000068	14.61	3540873	0.17	-0.13	0.12	fop_jk
22000069	19.53	3542574	3.59	-3.09	1.83	fop_deltaKp=DeltaJ
22000070	21.18	3547178	2.46	-2.18	-1.13	fop_j
22000071	16.71	3629330	1.13	0.77	0.83	roboAO_LP600
22000072	15.23	3632330	1.67	-1.63	-0.37	fop_j
22000073	13.37	3632418	0.75	0.57	-0.49	fop_j
22000074	19.50	3634051	0.61	-0.54	-0.29	fop_k
22000075	20.77	3641726	3.97	1.72	3.58	fop_j
22000076	16.39	3642335	0.33	-0.28	0.19	fop_gri
22000077	18.86	3648437	2.10	2.09	0.22	roboAO_LP600
22000078	18.47	3657758	9.19	-8.85	2.47	wolfgang_k
22000079	15.83	3660924	0.33	0.25	-0.22	roboAO_LP600

ID	Kp	hostID	sep	ΔRA	ΔDec	source
22000080	20.78	3662838	2.96	-0.46	-2.92	fop_j
22000081	16.65	3733628	0.93	-0.14	0.92	fop_i roboAO_LP600
22000082	17.65	3742855	3.14	1.88	2.51	fop_j
22000083	13.64	3742855	3.96	3.79	1.17	fop_j
22000084	14.93	3745690	0.10	0.02	-0.10	fop_692
22000085	15.55	3751118	1.05	0.99	-0.34	roboAO_LP600
22000086	21.31	3756801	1.47	-0.30	-1.44	fop_k
22000087	10.85	3834317	1.15	0.77	0.86	fop_692
22000088	19.95	3847138	3.82	-2.48	-2.91	fop_j
22000089	21.22	3858919	3.95	-0.43	-3.93	fop_j
22000090	17.01	3867615	0.94	-0.62	-0.71	fop_k
22000091	20.12	3936658	2.86	0.81	-2.74	fop_k
22000092	20.39	3937519	1.57	-1.56	0.20	fop_k
22000093	19.12	3937519	1.81	0.37	-1.77	fop_k
22000094	17.52	3968809	1.00	-0.29	0.96	fop_k
22000095	15.27	3969687	0.69	-0.50	-0.48	dressing fop_692 roboAO_LP600
22000096	16.91	4047631	9.30	0.26	-9.30	wolfgang_jhk
22000097	20.84	4047631	6.22	-3.29	-5.28	wolfgang_h
22000098	21.46	4047631	8.88	-8.32	3.09	wolfgang_h
22000099	12.53	4049901	2.16	2.12	0.45	fop_j roboAO_LP600
22000100	18.63	4055765	2.30	1.44	-1.79	fop_h
22000101	16.38	4075067	1.69	-0.19	-1.68	fop_i
22000102	16.51	4075067	1.88	-1.84	-0.42	fop_i
22000103	21.46	4135665	3.25	-0.34	-3.23	fop_j
22000104	14.91	4138557	1.62	1.52	-0.57	fop_i
22000105	17.64	4138557	2.92	-2.90	0.33	fop_i
22000106	16.35	4140813	0.33	0.31	-0.12	roboAO_LP600
22000107	13.64	4144236	0.56	-0.34	0.45	fop_692 roboAO_LP600
22000108	21.09	4157325	8.50	-6.29	-5.72	wolfgang_h
22000109	19.95	4157325	9.54	-8.01	-5.19	wolfgang_h wolfgang_k
22000110	13.05	4157325	9.98	-2.28	-9.71	wolfgang_k
22000111	19.84	4157325	7.17	4.98	-5.16	wolfgang_k
22000112	22.35	4175630	2.50	1.28	2.16	fop_j
22000113	18.77	4179201	0.66	0.66	0.00	fop_k
22000114	12.37	4247791	0.56	0.22	0.51	fop_LP562
22000115	18.04	4247991	1.03	0.97	0.35	fop_692
22000116	19.69	4247991	8.84	-6.87	5.57	wolfgang_h wolfgang_h
22000117	21.10	4247991	6.91	5.04	4.73	wolfgang_h
22000118	13.33	4253860	0.75	-0.72	0.19	roboAO_LP600
22000119	17.31	4255944	2.14	1.59	1.43	roboAO_LP600

ID	Kp	hostID	sep	ΔRA	ΔDec	source
22000120	20.22	4270253	3.42	-3.14	-1.33	fop_j
22000121	14.16	4276716	2.08	-1.48	-1.46	fop_jk roboAO_i wolfgang_jhk
22000122	19.64	4278221	2.86	-0.05	2.86	fop_j fop_k
22000123	19.73	4365645	2.01	0.94	-1.78	fop_h
22000124	20.04	4366323	3.59	0.34	3.57	fop_j
22000125	19.79	4366923	2.56	1.76	-1.85	fop_k
22000126	21.10	4372768	3.51	-1.62	-3.12	fop_j
22000127	20.65	4375101	3.56	-0.59	-3.52	fop_j
22000128	15.23	4446411	1.61	1.24	1.02	fop_j roboAO_LP600
22000129	16.05	4450844	0.81	-0.37	0.72	fop_692
22000130	16.68	4471747	1.06	-0.17	-1.05	roboAO_LP600
22000131	21.09	4476123	2.82	-2.29	-1.65	fop_j
22000132	21.09	4476123	2.84	0.76	2.73	fop_j
22000133	17.03	4476423	1.10	-0.06	-1.10	fop_i
22000134	19.72	4548011	2.93	-2.89	0.50	fop_k
22000135	20.60	4552729	2.07	-1.27	-1.63	fop_k
22000136	19.39	4567118	1.83	-1.66	-0.77	fop_jk
22000137	13.85	4571004	2.83	2.83	-0.14	fop_gri
22000138	18.56	4644604	1.82	-1.40	1.16	fop_i roboAO_i
22000139	14.68	4752451	0.36	0.22	0.28	fop_j
22000140	16.64	4764969	0.82	-0.52	0.64	fop_jk
22000141	21.80	4770174	6.81	3.63	-5.76	dressing
22000142	14.07	4770174	0.53	-0.26	-0.46	roboAO_LP600
22000143	20.06	4820550	2.33	1.98	1.23	fop_k
22000144	17.61	4830605	1.40	0.55	1.29	roboAO_LP600
22000145	11.06	4832225	0.93	0.82	0.43	fop_692
22000146	14.65	4832837	0.10	-0.04	-0.09	fop_k
22000147	20.75	4840513	3.90	-0.84	-3.80	fop_j
22000148	15.61	4840672	2.54	-1.23	-2.22	fop_j roboAO_LP600
22000149	17.12	4840672	4.03	2.25	-3.34	roboAO_LP600
22000150	18.38	4841374	0.67	0.21	0.64	fop_k
22000151	16.19	4846856	2.36	2.36	0.15	fop_j roboAO_LP600
22000152	21.05	4848424	4.05	4.05	-0.01	fop_j wolfgang_h
22000153	20.03	4848424	4.79	-4.74	-0.64	wolfgang_h
22000154	20.95	4848424	8.11	-7.73	-2.48	wolfgang_h
22000155	20.66	4851239	3.04	-1.16	-2.81	fop_k
22000156	15.71	4851356	2.20	-1.35	-1.74	fop_j
22000157	19.11	4851530	0.95	0.94	-0.10	fop_LP600 roboAO_LP600
22000158	20.95	4851530	3.68	-1.43	-3.39	fop_j
22000159	20.94	4858610	3.13	2.78	-1.44	fop_j

ID	Kp	hostID	sep	ΔRA	ΔDec	source
22000160	21.27	4861791	3.06	2.70	-1.44	fop_j
22000161	15.44	4862625	0.75	0.64	-0.40	roboAO_LP600
22000162	19.68	4862924	1.57	-1.52	-0.40	fop_jk
22000163	20.50	4863369	3.59	3.37	1.25	fop_j
22000164	20.12	4914423	2.47	2.38	0.64	adams_P fop_j
22000165	20.36	4914423	3.23	3.17	-0.60	fop_j
22000166	16.36	4915582	1.24	1.22	-0.19	roboAO_LP600
22000167	17.78	4917596	0.77	0.36	0.68	roboAO_LP600 wolfgang_jhk
22000168	21.70	4917596	8.74	-8.54	1.82	wolfgang_h
22000169	22.29	4917596	4.33	3.17	2.96	wolfgang_h
22000170	22.50	4917596	4.63	2.11	-4.13	wolfgang_h
22000171	21.51	4927315	3.65	2.52	-2.64	fop_j
22000172	20.17	4932442	8.78	5.19	7.08	wolfgang_h
22000173	20.91	4932442	9.40	-8.01	-4.92	wolfgang_h
22000174	14.76	4935172	1.13	1.05	0.42	roboAO_LP600
22000175	14.23	4939265	1.31	1.10	0.71	roboAO_LP600
22000176	20.83	4947726	3.82	-2.36	-3.01	fop_j
22000177	14.25	4950341	0.50	-0.50	0.02	fop_jk roboAO_LP600
22000178	15.31	4950557	1.41	-1.41	0.05	roboAO_LP600
22000179	15.54	5008245	1.20	0.67	0.99	roboAO_LP600
22000180	19.57	5020319	2.81	-0.23	2.80	fop_j
22000181	18.39	5021174	3.75	-1.26	-3.53	fop_deltaKp=DeltaJ
22000182	21.15	5022440	3.76	1.34	3.52	fop_j
22000183	17.22	5024252	2.49	-0.33	-2.47	fop_j
22000184	15.40	5024292	1.70	0.00	-1.70	fop_j
22000185	17.59	5024482	2.02	1.76	0.99	fop_j
22000186	17.88	5024482	3.67	3.34	-1.50	fop_j
22000187	20.60	5031882	3.40	-2.68	-2.09	fop_j
22000188	19.17	5039228	5.75	-2.92	4.95	wolfgang_k
22000189	20.72	5041569	2.82	0.33	-2.80	fop_j
22000190	18.45	5041569	9.79	-2.40	-9.50	wolfgang_jhk
22000191	19.54	5041569	8.97	-2.59	-8.58	wolfgang_jhk
22000192	19.90	5042210	2.80	-2.36	1.51	fop_h
22000193	20.68	5042785	3.33	3.14	1.09	fop_jk
22000194	22.00	5080636	3.15	-3.13	-0.36	wolfgang_k
22000195	21.46	5084942	9.97	6.30	7.73	wolfgang_h
22000196	20.40	5094751	2.03	1.83	-0.87	adams_P
22000197	21.20	5094751	5.27	-3.85	-3.59	adams_P
22000198	13.48	5096053	0.45	0.44	-0.10	roboAO_LP600
22000199	16.60	5103998	0.60	0.21	-0.56	roboAO_LP600

ID	Kp	hostID	sep	ΔRA	ΔDec	source
22000200	13.83	5121511	0.43	0.38	-0.21	fop_692 roboAO_i wolfgang_jhk
22000201	18.59	5121511	8.26	-2.36	-7.91	wolfgang_j
22000202	13.85	5121511	0.43	-0.37	0.22	wolfgang_jhk
22000203	18.31	5129453	0.99	-0.80	-0.58	roboAO_LP600
22000204	20.37	5130563	3.81	1.68	3.42	fop_j
22000205	18.40	5185897	4.58	4.03	-2.18	dressing
22000206	17.66	5195945	2.13	-2.07	-0.49	fop_i
22000207	16.40	5196851	1.58	0.14	-1.57	roboAO_LP600
22000208	18.43	5202905	0.53	0.48	-0.23	fop_jhk
22000209	17.50	5213404	1.49	1.33	-0.68	roboAO_LP600
22000210	18.12	5215508	2.52	1.66	1.90	fop_jk
22000211	18.28	5215508	3.02	-1.01	-2.85	fop_jk
22000212	13.58	5216727	2.64	2.35	1.22	fop_j
22000213	14.01	5253802	1.74	-1.65	-0.56	fop_j roboAO_LP600
22000214	19.82	5260419	1.22	-0.82	-0.91	roboAO_LP600
22000215	13.76	5272233	0.52	0.28	-0.44	roboAO_LP600
22000216	19.37	5272878	1.07	-0.47	-0.96	wolfgang_k
22000217	19.97	5282477	2.35	0.25	-2.33	fop_j
22000218	19.35	5294945	2.74	2.69	0.52	roboAO_LP600
22000219	15.67	5301750	0.18	0.13	-0.13	fop_gri
22000220	22.98	5301750	3.94	-2.09	-3.34	fop_gri
22000221	18.32	5301955	2.20	1.10	1.91	roboAO_LP600
22000222	20.86	5303557	1.45	1.42	0.30	fop_j
22000223	14.49	5309353	2.19	-2.17	0.26	fop_j
22000224	17.76	5357545	6.72	-4.75	-4.76	wolfgang_h
22000225	20.72	5357545	8.58	-4.52	-7.29	wolfgang_h
22000226	18.89	5357545	4.59	-3.88	-2.45	wolfgang_h
22000227	17.73	5358241	0.11	-0.09	-0.05	fop_gri
22000228	21.22	5364071	2.25	1.23	-1.89	fop_k
22000229	15.50	5374854	2.90	2.19	1.90	fop_j roboAO_LP600
22000230	20.53	5376067	2.76	0.25	2.75	fop_j
22000231	18.10	5383248	5.42	4.92	2.27	adams_A
22000232	16.05	5384713	1.10	0.17	1.08	fop_jk roboAO_LP600
22000233	17.44	5384713	3.53	-3.51	-0.41	fop_gri roboAO_LP600
22000234	15.80	5385410	1.12	1.11	-0.12	roboAO_LP600
22000235	20.43	5392702	3.77	-1.75	3.34	fop_j
22000236	18.97	5398002	1.00	-0.56	-0.83	fop_k
22000237	21.03	5436338	5.27	1.91	-4.91	wolfgang_h
22000238	22.00	5450893	5.80	-3.22	4.83	dressing
22000239	15.80	5473556	2.78	2.09	-1.84	dressing

ID	Kp	hostID	sep	ΔRA	ΔDec	source
22000240	21.20	5473556	4.29	-1.66	-3.96	dressing
22000241	20.80	5473556	4.82	-4.15	2.45	dressing
22000242	18.80	5473556	9.77	-0.70	9.74	dressing
22000243	19.20	5473556	8.17	8.13	0.81	dressing
22000244	15.50	5475431	0.60	0.60	0.03	fop_i roboAO_LP600
22000245	20.74	5477805	3.92	2.42	-3.09	fop_j
22000246	20.89	5478083	2.60	-2.58	-0.30	fop_j
22000247	10.89	5513648	0.12	0.11	-0.05	fop_692
22000248	19.10	5514383	4.44	4.07	-1.77	wolfgang_jhk
22000249	18.33	5526717	0.60	0.21	-0.56	dressing fop_LP600 roboAO_LP600
22000250	16.82	5531953	0.15	0.09	-0.11	fop_692
22000251	21.80	5551228	3.35	3.08	-1.32	fop_j
22000252	19.58	5553959	1.45	1.23	0.77	roboAO_LP600
22000253	16.48	5562090	1.17	1.17	0.00	roboAO_LP600
22000254	15.58	5564082	2.29	-1.65	1.59	fop_jk
22000255	10.74	5598639	0.77	-0.47	0.61	roboAO_LP600
22000256	20.90	5601258	1.73	-1.39	-1.04	fop_gri
22000257	20.35	5617854	4.84	0.87	-4.76	wolfgang_k
22000258	15.52	5629353	1.23	1.23	-0.02	roboAO_LP600
22000259	18.02	5633259	1.73	1.72	0.18	roboAO_LP600
22000260	20.90	5636642	2.18	1.00	1.94	fop_j
22000261	18.74	5644412	2.17	-2.04	0.74	roboAO_LP600
22000262	21.12	5649206	3.66	3.57	0.79	fop_j
22000263	21.46	5649215	3.07	-0.66	2.99	fop_j
22000264	17.05	5649836	2.00	-0.74	1.86	fop_j
22000265	14.34	5652893	0.25	0.19	-0.17	dressing fop_k
22000266	19.70	5652893	5.30	0.63	5.27	dressing
22000267	17.51	5705819	1.30	-0.75	-1.06	roboAO_LP600
22000268	17.60	5706966	1.27	-1.25	-0.23	fop_h roboAO_i
22000269	12.36	5717567	0.09	0.09	-0.02	fop_k
22000270	20.70	5735762	4.39	4.18	-1.33	adams_P
22000271	20.93	5769943	3.09	2.49	1.84	fop_j
22000272	15.53	5771719	0.21	0.20	-0.05	fop_692 roboAO_LP600
22000273	17.09	5780885	1.90	1.85	-0.43	adams_A fop_jk roboAO_i
22000274	20.58	5787131	3.10	2.90	-1.10	fop_j
22000275	18.50	5787131	1.39	0.82	1.12	roboAO_LP600
22000276	21.88	5793275	3.15	0.92	3.01	fop_k
22000277	15.40	5796675	1.25	-1.25	0.06	fop_jk fop_jk roboAO_LP600 wolfgang_jhk
22000278	16.84	5796675	6.61	-1.02	6.53	wolfgang_jhk

ID	Kp	hostID	sep	ΔRA	ΔDec	source
22000279	18.59	5796675	8.29	-1.08	-8.22	wolfgang_jhk
22000280	15.71	5801571	0.53	-0.20	0.49	roboAO_LP600
22000281	20.08	5866724	2.90	2.41	1.62	fop_k
22000282	19.91	5876360	2.19	1.65	1.44	fop_j
22000283	20.58	5894073	3.83	-3.80	-0.48	fop_j
22000284	21.60	5897826	4.08	-0.87	3.99	adams_P
22000285	14.08	5897826	0.34	0.20	0.28	roboAO_LP600
22000286	21.70	5903312	5.84	0.65	-5.80	adams_P
22000287	15.47	5903749	0.27	-0.26	-0.01	roboAO_LP600 wolfgang_h
22000288	20.67	5903749	1.69	-0.13	1.69	wolfgang_h
22000289	20.63	5903749	9.57	-6.51	-7.01	wolfgang_h
22000290	21.07	5903749	9.39	9.07	-2.41	wolfgang_h
22000291	20.17	5903749	9.98	0.99	-9.93	wolfgang_h
22000292	20.52	5903749	8.47	-4.64	7.09	wolfgang_h
22000293	20.87	5903749	5.63	-5.07	-2.45	wolfgang_h
22000294	21.57	5903749	3.96	-3.83	-1.02	wolfgang_h
22000295	21.60	5903749	6.38	0.35	-6.37	wolfgang_h
22000296	21.88	5903749	8.55	0.77	8.51	wolfgang_h
22000297	21.97	5903749	4.76	-3.69	3.00	wolfgang_h
22000298	22.27	5903749	6.40	-6.15	1.74	wolfgang_h
22000299	15.12	5946568	0.08	0.08	-0.00	fop_692
22000300	19.50	5966322	5.79	5.78	-0.38	adams_P
22000301	18.08	5972334	1.68	1.67	-0.15	fop_LP600 roboAO_LP600
22000302	16.18	5977470	1.05	0.63	-0.84	fop_692
22000303	20.39	5985713	2.16	0.47	-2.11	fop_k
22000304	19.44	5986270	2.83	2.68	-0.92	roboAO_LP600
22000305	20.86	5991765	3.74	-0.33	3.72	fop_j
22000306	12.29	6021275	0.91	0.90	-0.11	fop_692 roboAO_LP600 wolfgang_jhk
22000307	22.33	6026438	1.29	0.74	1.05	fop_gri
22000308	15.71	6037187	1.22	0.75	0.96	roboAO_LP600
22000309	16.33	6037581	0.27	0.16	-0.22	fop_LP600 roboAO_LP600
22000310	16.36	6046311	1.41	-0.36	-1.36	roboAO_LP600
22000311	14.93	6046540	0.30	0.21	0.22	roboAO_LP600
22000312	18.38	6047853	1.75	-0.60	-1.64	roboAO_LP600
22000313	16.39	6056992	3.51	1.14	-3.32	roboAO_LP600
22000314	16.28	6058875	1.28	0.68	1.09	fop_deltaKp=DeltaZ
22000315	18.17	6062088	1.92	-1.67	-0.94	fop_i
22000316	15.70	6066379	0.73	-0.42	-0.59	fop_i roboAO_LP600
22000317	20.19	6067545	1.94	-1.89	0.45	fop_k
22000318	20.63	6071903	4.56	-2.51	3.81	adams_P wolfgang_jhk

ID	Kp	hostID	sep	ΔRA	ΔDec	source
22000319	15.99	6071903	2.07	-1.87	-0.89	adams_P fop_jk roboAO_i wolfgang_jhk
22000320	18.59	6071903	9.18	-8.89	-2.26	wolfgang_jhk
22000321	20.10	6071903	9.45	7.08	6.25	wolfgang_j
22000322	20.97	6103377	3.77	-0.82	-3.68	fop_j
22000323	13.71	6143819	2.22	1.63	-1.50	fop_j
22000324	21.30	6144039	2.16	1.74	1.28	fop_k
22000325	20.18	6144039	3.76	0.00	3.76	fop_j
22000326	12.92	6145939	0.77	0.23	0.74	roboAO_LP600
22000327	24.33	6149553	3.49	-3.44	-0.55	fop_gri
22000328	22.28	6149553	3.87	-0.98	3.75	fop_gri
22000329	16.73	6183511	0.88	0.33	0.82	roboAO_LP600
22000330	15.77	6185476	0.31	-0.29	-0.11	fop_692
22000331	21.69	6185496	3.61	-2.22	2.84	fop_j
22000332	16.62	6196457	1.48	1.00	-1.09	adams_P fop_jk roboAO_LP600
22000333	20.04	6196457	2.33	1.06	2.08	fop_jk
22000334	14.40	6197344	2.48	-1.48	1.99	fop_j
22000335	15.61	6197344	2.45	1.47	-1.96	roboAO_LP600
22000336	19.42	6198999	2.11	-1.02	-1.85	roboAO_LP600
22000337	20.07	6209225	0.94	0.51	0.79	fop_jk
22000338	20.88	6209347	3.35	1.72	-2.87	fop_j
22000339	20.75	6227560	3.25	-3.21	-0.54	fop_j
22000340	20.05	6263468	2.41	0.08	-2.40	fop_j
22000341	15.68	6263593	0.47	-0.14	-0.45	fop_gri
22000342	20.98	6263593	0.76	-0.19	-0.73	fop_gri
22000343	22.64	6263593	1.21	-1.17	-0.31	fop_gri
22000344	20.09	6263593	1.22	0.69	1.01	fop_gri
22000345	21.13	6263593	2.95	-1.08	2.74	fop_gri
22000346	12.33	6268648	0.21	-0.02	-0.21	fop_692 roboAO_deltaiEqDeltaKp
22000347	12.12	6278762	1.97	-1.89	-0.56	fop_jk roboAO_LP600
22000348	20.29	6279974	2.69	2.46	-1.10	fop_i
22000349	13.05	6289257	0.08	-0.07	-0.03	fop_692
22000350	20.21	6309763	3.44	3.20	1.27	fop_j
22000351	21.11	6312314	3.73	2.96	-2.28	fop_j
22000352	20.59	6345732	8.66	-8.50	1.63	wolfgang_h
22000353	13.15	6364582	0.04	0.01	0.04	fop_deltaKp=Delta880
22000354	22.04	6382217	9.79	9.47	2.48	wolfgang_h
22000355	21.05	6382217	9.89	-9.76	1.57	wolfgang_h
22000356	22.47	6382217	8.51	-6.65	-5.31	wolfgang_h
22000357	22.71	6382217	9.39	-2.67	9.01	wolfgang_h

ID	Kp	hostID	sep	ΔRA	ΔDec	source
22000358	23.00	6382217	6.17	-2.54	-5.62	wolfgang_h
22000359	20.22	6387450	3.31	1.88	2.72	fop_j
22000360	19.67	6425957	3.14	2.80	1.43	fop_j
22000361	15.28	6428942	1.04	-0.37	0.97	roboAO_LP600
22000362	17.54	6451936	1.28	1.07	-0.70	fop_LP600 roboAO_LP600
22000363	19.50	6467363	8.22	-0.85	-8.18	dressing
22000364	21.15	6470149	2.81	2.66	-0.92	fop_i
22000365	21.44	6471021	2.49	0.94	-2.31	fop_k
22000366	20.91	6471021	3.56	2.98	1.94	fop_k
22000367	18.03	6497146	0.44	-0.10	-0.43	fop_692
22000368	20.69	6515335	2.82	-2.62	1.06	fop_j
22000369	17.15	6515722	1.84	-1.84	0.03	wolfgang_k
22000370	20.35	6520519	3.67	-1.39	-3.39	fop_j
22000371	15.54	6521045	1.83	-1.62	-0.86	fop_i
22000372	17.97	6523058	0.75	0.39	-0.64	roboAO_LP600
22000373	20.10	6523351	2.61	-2.50	0.74	dressing fop_k
22000374	18.46	6525946	2.08	-0.29	2.06	roboAO_LP600
22000375	11.46	6528464	0.10	0.09	0.04	adams_A fop_692
22000376	18.75	6541920	1.36	0.00	-1.36	fop_k
22000377	18.95	6543682	1.94	1.40	-1.35	roboAO_LP600
22000378	20.80	6545051	3.58	-3.43	-1.02	fop_j
22000379	21.23	6551106	3.45	2.86	1.92	fop_j
22000380	18.40	6607357	1.75	-0.52	-1.67	dressing fop_k roboAO_LP600 wolfgang_hk
22000381	21.15	6607357	9.73	4.08	8.84	wolfgang_h
22000382	20.22	6607357	8.54	-4.59	7.20	wolfgang_h
22000383	20.25	6607357	8.75	8.51	-2.02	wolfgang_h
22000384	21.02	6607357	5.02	-1.55	4.77	wolfgang_h
22000385	20.19	6614926	3.84	-3.42	-1.73	fop_j
22000386	20.71	6672229	3.61	-0.98	-3.47	fop_j
22000387	19.28	6675060	2.30	-2.30	-0.12	roboAO_LP600
22000388	18.80	6678383	1.86	-0.20	-1.85	fop_i
22000389	16.08	6679295	0.68	0.23	0.64	roboAO_LP600
22000390	21.14	6690082	2.69	0.72	2.59	fop_h
22000391	15.92	6697605	0.39	-0.27	-0.29	roboAO_LP600
22000392	20.75	6697976	2.44	1.82	1.63	fop_k
22000393	20.83	6715997	3.97	-3.75	1.29	fop_j
22000394	16.70	6717252	1.22	1.18	-0.32	roboAO_LP600
22000395	18.23	6719086	9.75	8.03	-5.53	wolfgang_k
22000396	17.43	6752502	2.94	2.11	-2.04	fop_j

ID	Kp	hostID	sep	ΔRA	ΔDec	source
22000397	17.76	6766634	0.77	-0.77	-0.01	fop_jk roboAO_i
22000398	16.17	6767227	0.96	-0.44	0.86	roboAO_LP600
22000399	20.23	6767337	2.86	-2.86	0.06	fop_jk
22000400	19.24	6776555	1.88	-0.97	-1.61	roboAO_LP600
22000401	19.88	6779260	8.13	4.55	-6.73	dressing wolfgang_jh
22000402	19.98	6779260	3.31	1.43	2.99	wolfgang_jh
22000403	13.76	6803202	0.24	-0.14	-0.19	fop_692 roboAO_i wolfgang_k
22000404	14.39	6803855	0.31	-0.18	-0.25	roboAO_LP600
22000405	19.53	6805146	3.82	1.22	3.63	fop_j
22000406	13.18	6851425	1.22	-0.68	-1.01	roboAO_LP600
22000407	16.90	6878240	1.10	0.47	-1.00	fop_k roboAO_LP600
22000408	14.38	6880123	1.31	1.30	0.14	fop_j
22000409	22.21	6922244	3.08	-3.08	-0.23	adams_P fop_j
22000410	20.53	6922244	3.79	3.78	0.05	adams_P fop_j
22000411	22.39	6928906	4.00	-3.40	-2.11	dressing fop_k
22000412	18.65	6945786	1.83	-1.55	-0.97	roboAO_LP600
22000413	19.03	6946199	1.43	-0.65	1.27	fop_LP600 roboAO_LP600
22000414	20.38	6946199	3.82	0.49	-3.79	fop_j
22000415	20.64	6946708	2.69	2.13	-1.65	fop_k
22000416	17.82	6952570	1.24	-0.75	-0.99	roboAO_LP600
22000417	17.98	6960913	0.47	-0.34	0.32	fop_jk
22000418	20.54	7031208	3.24	2.51	-2.05	fop_j
22000419	19.90	7032421	9.92	-6.48	-7.51	wolfgang_h
22000420	19.71	7032687	2.50	-2.19	1.22	fop_j
22000421	15.15	7047922	1.84	-0.57	1.75	fop_j roboAO_LP600
22000422	19.04	7050989	3.00	2.91	-0.70	fop_jk
22000423	13.70	7051984	0.43	0.40	-0.15	dressing fop_692
22000424	14.55	7097965	0.26	0.02	-0.26	roboAO_LP600
22000425	16.88	7098355	1.49	-0.61	-1.36	roboAO_LP600
22000427	20.48	7132798	3.61	-2.91	2.14	fop_j
22000428	20.37	7135852	1.32	-1.31	0.16	wolfgang_hk
22000429	18.74	7137213	1.58	0.47	-1.51	fop_jhk roboAO_LP600
22000430	14.43	7138841	1.82	-0.65	-1.70	fop_j
22000431	17.67	7183745	7.68	6.37	-4.30	wolfgang_jhk
22000432	15.54	7220429	0.29	-0.27	0.09	roboAO_LP600
22000433	21.84	7259249	3.88	2.10	-3.27	fop_j
22000434	15.78	7273277	0.81	-0.18	-0.79	fop_k roboAO_i
22000435	20.40	7285757	3.72	0.32	3.71	fop_j
22000436	17.56	7295235	7.94	0.45	7.93	wolfgang_k
22000437	21.38	7296094	3.80	-2.74	2.64	fop_deltaKp=DeltaJ

ID	Kp	hostID	sep	ΔRA	ΔDec	source
22000438	18.60	7296438	5.73	4.69	-3.29	adams_P
22000439	11.45	7296438	0.09	0.09	-0.02	fop_692
22000440	20.36	7362632	3.40	1.28	-3.15	fop_j
22000441	20.28	7365447	3.73	-2.58	-2.70	fop_j
22000442	19.30	7375348	3.62	2.11	2.94	adams_A
22000443	20.32	7428316	3.84	1.05	-3.69	fop_j
22000444	14.53	7446631	1.09	1.05	0.28	roboAO_LP600
22000445	14.35	7449136	0.41	0.25	-0.32	fop_692 roboAO_i wolfgang_k
22000446	19.11	7449136	8.16	-8.16	-0.12	wolfgang_j
22000447	18.49	7450747	1.66	-0.40	-1.61	roboAO_LP600
22000448	25.36	7455287	3.09	0.06	-3.09	fop_gri
22000449	17.56	7457278	1.63	1.53	-0.56	fop_k
22000450	17.52	7531677	1.44	-1.28	0.65	roboAO_LP600
22000451	18.11	7539277	0.70	-0.13	0.69	fop_k
22000452	21.36	7543649	3.84	3.69	1.07	fop_j
22000453	20.35	7582691	3.88	3.36	-1.94	fop_j
22000454	20.12	7605600	3.20	0.96	3.05	fop_j
22000455	20.67	7620844	3.16	-0.16	3.16	fop_j
22000456	13.36	7622486	0.44	-0.21	-0.39	roboAO_LP600
22000457	14.53	7630658	1.78	-0.80	1.59	fop_j
22000458	20.59	7631138	3.32	0.59	3.27	fop_k
22000459	20.83	7631138	3.97	-3.39	-2.07	fop_k
22000460	19.48	7670943	2.61	2.51	0.70	fop_k
22000461	15.43	7672940	0.22	0.09	0.20	fop_jk fop_692
22000462	16.61	7684873	1.72	-1.72	0.11	fop_jk
22000463	20.46	7692248	2.75	-1.76	2.12	fop_j
22000464	14.53	7694615	1.45	0.16	1.44	fop_j
22000465	17.28	7730747	0.20	0.00	0.20	fop_692
22000466	15.60	7731281	0.44	-0.27	-0.35	fop_k
22000467	17.71	7746958	2.91	1.38	2.56	fop_i
22000468	14.16	7746958	5.38	-5.38	-0.21	wolfgang_jk
22000469	16.54	7746958	6.85	1.62	6.66	wolfgang_jhk
22000470	20.35	7748487	3.68	-3.59	-0.82	fop_j
22000471	20.75	7778767	3.84	-2.79	-2.64	fop_j
22000472	18.65	7802719	1.91	-0.24	1.89	fop_k roboAO_LP600
22000473	20.95	7811397	3.17	1.83	2.58	fop_j
22000474	16.74	7868967	2.58	2.08	-1.52	fop_j roboAO_LP600
22000475	21.17	7871954	9.17	3.93	-8.29	wolfgang_h
22000476	16.24	7877978	0.38	0.22	-0.30	fop_692 roboAO_LP600
22000477	13.52	7887791	0.39	0.00	0.39	fop_692 wolfgang_jhk

ID	Kp	hostID	sep	ΔRA	ΔDec	source
22000478	21.22	7898352	3.66	-3.66	0.19	fop_j
22000479	18.04	7905106	2.71	-2.14	1.67	roboAO_LP600
22000480	15.03	7905106	3.58	-3.42	1.07	fop_j roboAO_LP600
22000481	23.53	7907423	2.22	0.80	2.07	fop_gri
22000482	23.20	7907423	3.05	-1.87	-2.41	fop_gri
22000483	16.33	7918478	0.96	-0.38	-0.88	roboAO_LP600
22000484	17.09	7949593	0.67	0.05	0.67	roboAO_LP600
22000485	20.07	7960295	2.84	-0.56	2.79	fop_deltaKp=DeltaJ
22000486	15.96	7976520	0.70	0.16	0.68	fop_i roboAO_i
22000487	15.69	7976520	8.04	8.03	0.16	wolfgang_k
22000488	13.14	7983117	0.48	-0.32	0.36	fop_692 roboAO_LP600
22000489	14.39	7983117	1.34	-0.40	-1.28	fop_h roboAO_LP600
22000490	12.85	8005002	1.34	1.03	-0.85	fop_j
22000491	17.46	8007675	2.15	-1.71	1.29	fop_jk
22000492	20.12	8026752	2.53	0.19	2.52	wolfgang_k
22000493	15.21	8046659	1.61	-0.63	1.48	fop_j
22000494	16.06	8073705	1.55	-0.12	-1.55	fop_692 roboAO_LP600
22000495	13.62	8074328	0.24	0.21	0.11	fop_i roboAO_i
22000496	17.34	8074328	6.07	6.04	0.65	wolfgang_k
22000497	16.90	8081899	8.76	4.34	-7.61	dressing
22000498	14.82	8087812	0.89	0.60	-0.66	roboAO_LP600
22000499	14.56	8096395	0.40	0.00	-0.40	fop_jk
22000500	14.36	8107380	0.28	0.25	-0.14	fop_LP600 roboAO_LP600 wolfgang_k
22000501	19.44	8107380	7.44	5.93	-4.48	wolfgang_h
22000502	19.51	8142787	1.96	-1.63	-1.09	fop_k
22000503	18.08	8142942	8.55	6.87	-5.08	wolfgang_k
22000504	16.64	8158429	0.62	-0.62	-0.00	roboAO_LP600
22000505	20.92	8160953	6.89	-6.50	2.29	wolfgang_h
22000506	16.18	8161561	1.71	1.08	-1.33	fop_LP600 roboAO_LP600
22000507	18.45	8179973	2.50	-2.30	-0.97	fop_k
22000508	19.07	8179973	3.09	-1.29	2.81	fop_k fop_k
22000509	19.78	8179973	3.20	3.02	-1.07	fop_k
22000510	14.87	8183288	0.18	-0.07	0.16	fop_692
22000511	18.88	8191672	0.91	0.20	-0.88	adams_P fop_j
22000512	20.78	8192861	2.97	-2.05	2.14	fop_j
22000513	15.23	8196226	0.35	-0.35	0.03	roboAO_LP600
22000514	13.30	8197406	0.34	-0.15	0.30	roboAO_LP600
22000515	20.97	8197560	3.49	-0.55	3.45	fop_j
22000516	14.97	8222627	0.78	0.08	-0.78	roboAO_LP600

ID	Kp	hostID	sep	ΔRA	ΔDec	source
22000517	14.94	8240617	0.59	-0.58	0.11	fop_692 roboAO_LP600
22000518	14.96	8241079	0.38	-0.38	0.02	fop_692 roboAO_LP600
22000519	19.81	8260218	1.69	-0.71	-1.53	roboAO_LP600
22000520	15.49	8261920	0.89	-0.65	-0.61	fop_j roboAO_LP600
22000521	19.77	8261920	1.52	-1.29	-0.81	wolfgang_hk
22000522	17.00	8261920	3.89	2.87	-2.62	wolfgang_hk
22000523	17.11	8261920	3.90	2.23	-3.20	wolfgang_hk
22000524	17.21	8261920	9.48	9.08	-2.72	wolfgang_hk
22000525	22.78	8261920	9.43	6.01	-7.27	wolfgang_h
22000526	21.34	8261920	8.54	1.14	-8.46	wolfgang_hk
22000527	21.86	8261920	5.63	-5.22	2.11	wolfgang_h
22000528	22.46	8261920	4.60	3.02	3.47	wolfgang_h
22000529	22.74	8261920	9.90	9.78	1.52	wolfgang_h
22000530	21.41	8261920	2.98	-0.94	-2.82	wolfgang_k
22000531	20.60	8263545	3.95	3.63	-1.56	fop_j
22000532	20.88	8265520	3.46	-1.34	-3.19	fop_j
22000533	15.17	8278371	0.39	-0.24	0.31	fop_692 roboAO_i wolfgang_k
22000534	16.54	8280511	0.75	-0.59	0.47	fop_k roboAO_i
22000535	21.47	8331612	3.03	-2.05	2.24	fop_j
22000536	20.24	8331612	3.40	2.44	-2.36	fop_j
22000537	16.24	8332521	1.32	0.81	-1.04	fop_k roboAO_LP600
22000538	14.85	8332986	0.75	-0.22	-0.72	roboAO_LP600
22000539	13.41	8345384	0.11	-0.02	0.10	fop_692
22000540	16.96	8345384	2.14	0.63	2.04	fop_k roboAO_LP600
22000541	20.55	8364969	3.78	-3.22	-1.99	fop_j
22000542	20.38	8374499	3.75	1.26	3.53	fop_j
22000543	20.70	8378922	3.77	3.14	2.09	fop_j
22000544	18.04	8394475	2.12	-1.93	-0.88	fop_k
22000545	17.71	8394475	3.08	-0.36	-3.06	fop_k fop_j
22000546	20.36	8394721	2.49	1.23	2.17	fop_k
22000547	21.06	8396288	3.92	1.97	3.39	fop_j
22000548	16.97	8396660	2.64	-2.00	1.73	fop_k
22000549	21.65	8397446	3.59	-0.39	3.57	fop_j
22000550	20.87	8397947	3.70	-3.61	0.82	fop_h
22000551	20.04	8398290	2.28	1.05	-2.02	fop_k
22000552	14.62	8424002	0.78	0.08	-0.78	roboAO_LP600
22000553	18.97	8429817	2.36	-2.09	1.10	fop_jk
22000554	19.95	8429817	2.67	2.43	-1.10	fop_jk
22000555	20.70	8456679	5.45	-3.97	-3.73	adams_P
22000556	20.01	8463346	0.40	-0.07	0.40	fop_k

ID	Kp	hostID	sep	ΔRA	ΔDec	source
22000557	19.99	8505215	3.48	2.62	2.28	fop_gri
22000558	16.21	8546542	1.30	0.23	1.28	roboAO_LP600
22000559	13.68	8552719	0.50	-0.46	0.20	fop_692 roboAO_LP600
22000560	14.70	8554498	0.14	-0.12	0.08	fop_692
22000561	14.23	8570210	0.08	-0.08	0.02	fop_LP562
22000562	18.77	8581240	3.33	-3.21	-0.89	fop_k
22000563	17.80	8636333	0.31	-0.31	-0.02	fop_k
22000564	16.04	8639908	6.80	-5.68	3.73	wolfgang_k
22000565	21.90	8644288	4.80	-1.60	4.52	adams_P
22000566	21.50	8644288	4.98	3.44	-3.60	adams_P
22000567	22.20	8644288	5.72	5.48	1.63	adams_P
22000568	18.06	8644911	0.97	-0.23	0.94	roboAO_LP600
22000569	17.91	8652577	1.50	1.31	0.72	fop_jk
22000570	20.32	8652577	2.04	-2.02	-0.21	fop_jk
22000571	21.92	8652577	3.96	0.59	3.92	fop_jk
22000572	16.99	8656535	3.24	0.98	-3.09	fop_j roboAO_LP600
22000573	18.66	8656535	3.18	-2.94	-1.20	fop_j roboAO_LP600
22000574	15.28	8669092	0.72	-0.69	-0.18	adams_A adams_P fop_692
22000575	16.20	8669092	2.73	-2.60	-0.83	adams_A
22000576	20.50	8669092	2.72	-2.65	-0.63	adams_P fop_j
22000577	21.08	8676038	4.60	-2.28	4.00	wolfgang_h
22000578	19.72	8680979	2.09	-1.05	-1.81	fop_LP600 roboAO_LP600
22000579	19.31	8686097	1.83	1.83	0.07	fop_k
22000580	15.77	8687088	0.40	0.35	-0.20	fop_k
22000581	20.53	8689793	3.11	-2.02	2.36	fop_j
22000582	12.69	8703887	1.07	0.54	0.92	fop_692
22000583	16.04	8711794	0.84	0.33	-0.77	fop_h
22000584	16.40	8738775	0.66	0.61	-0.26	roboAO_LP600
22000585	15.14	8747910	0.13	-0.07	-0.11	fop_jk
22000586	18.94	8747910	2.05	-1.71	-1.13	fop_j roboAO_LP600
22000587	21.30	8750043	3.07	-2.66	1.53	fop_h
22000588	18.42	8765560	1.05	-0.91	-0.53	roboAO_LP600
22000589	18.65	8765560	2.01	1.40	-1.45	roboAO_LP600
22000590	18.21	8766285	1.85	1.40	1.21	fop_j
22000591	18.64	8766285	3.11	-3.11	0.01	fop_j
22000592	18.41	8766650	9.15	-8.94	1.95	wolfgang_h
22000593	18.94	8766650	8.11	-7.65	2.68	wolfgang_h
22000594	16.40	8800954	1.09	-0.96	-0.52	fop_k roboAO_i wolfgang_hk
22000595	15.56	8804397	0.97	0.79	-0.55	fop_692
22000596	16.35	8805348	1.96	-1.43	-1.34	fop_i

ID	Kp	hostID	sep	ΔRA	ΔDec	source
22000597	18.24	8826878	8.44	6.11	-5.83	wolfgang_k
22000598	19.61	8836224	3.90	3.26	-2.14	fop_j
22000599	15.09	8838950	1.16	-1.08	0.40	dressing fop_k roboAO_LP600
22000600	20.70	8838950	7.77	5.55	5.44	dressing
22000601	15.23	8847111	1.71	1.57	-0.67	fop_j
22000602	11.05	8848288	0.46	0.41	-0.20	fop_k roboAO_i
22000603	12.54	8866102	1.67	1.00	1.34	adams_A fop_LP562 roboAO_LP600
22000604	13.69	8878187	0.66	-0.54	-0.38	fop_jk
22000605	17.11	8883593	4.59	-3.40	3.08	wolfgang_k
22000606	24.00	8890150	3.12	2.56	-1.78	fop_gri
22000607	20.75	8890150	5.94	1.09	5.83	wolfgang_jhk
22000608	17.27	8892303	1.09	-0.46	-0.99	roboAO_LP600
22000609	16.40	8894646	1.42	-0.79	-1.18	fop_LP600 roboAO_LP600
22000610	16.17	8895758	0.30	-0.05	-0.30	roboAO_LP600
22000611	20.14	8916492	2.36	-1.17	-2.05	fop_k
22000612	18.05	8948424	1.87	1.74	0.70	fop_j
22000613	21.04	8950568	1.81	-1.41	1.13	wolfgang_h
22000614	20.85	8950568	7.86	-7.71	-1.55	wolfgang_h
22000615	21.01	8950568	4.40	0.35	-4.39	wolfgang_h
22000616	21.25	8950568	9.99	9.96	-0.83	wolfgang_h
22000617	20.67	8955709	3.45	-3.33	0.89	fop_j
22000618	20.57	8955709	3.71	1.86	-3.21	fop_j
22000619	23.86	8973129	1.77	-1.30	1.21	fop_gri
22000620	18.67	9002278	2.82	2.68	-0.87	fop_j
22000621	20.32	9007151	3.64	0.60	-3.59	fop_k
22000622	16.60	9017682	1.68	-0.20	-1.67	fop_j roboAO_LP600
22000623	17.20	9025922	3.34	3.32	0.37	fop_j
22000624	19.26	9026007	0.66	-0.57	-0.33	fop_k
22000625	19.69	9101496	0.95	-0.95	0.05	wolfgang_k
22000626	19.30	9109857	7.22	5.06	-5.15	dressing
22000627	14.76	9116510	1.38	1.09	0.86	fop_j
22000628	18.23	9146018	1.83	1.25	-1.34	roboAO_LP600
22000629	18.84	9150827	2.39	0.93	-2.20	fop_h
22000630	21.27	9150827	3.38	0.13	3.38	fop_h
22000631	18.69	9162741	1.91	1.06	1.59	fop_j
22000632	18.67	9166862	1.38	0.07	-1.38	roboAO_LP600
22000633	16.44	9171801	2.03	-0.92	-1.81	fop_j
22000634	21.39	9177629	8.06	-7.57	2.78	wolfgang_h
22000635	19.36	9209624	1.39	0.41	-1.33	fop_LP600 roboAO_LP600
22000636	14.99	9266285	2.16	2.15	-0.22	fop_deltaKp=DeltaV

ID	Kp	hostID	sep	ΔRA	ΔDec	source
22000637	17.31	9266431	1.64	0.02	-1.64	fop_i
22000638	13.14	9283156	0.73	0.55	-0.48	fop_LP600 roboAO_LP600
22000639	15.41	9334893	1.50	-0.38	-1.45	dressing fop_k roboAO_LP600
22000640	19.19	9349482	8.37	-2.91	7.84	wolfgang_h
22000641	14.13	9389245	0.77	-0.47	0.61	roboAO_i
22000642	15.42	9394605	1.93	1.68	0.96	fop_j
22000643	14.57	9405541	2.26	2.10	0.86	fop_i
22000644	19.50	9412760	9.79	-3.93	8.96	dressing
22000645	13.78	9412760	0.08	0.08	0.02	fop_k
22000646	16.19	9427402	8.62	5.99	6.20	wolfgang_k
22000647	20.22	9427402	6.42	4.28	4.79	wolfgang_k
22000648	20.59	9455677	3.85	-3.81	-0.52	fop_j
22000649	12.96	9471974	1.05	0.92	-0.50	fop_jk roboAO_i wolfgang_jhk
22000650	16.92	9471974	9.57	-4.80	-8.28	wolfgang_jhk
22000651	18.85	9471974	8.09	-8.09	-0.07	wolfgang_j
22000652	20.42	9472328	3.23	1.98	2.55	fop_j
22000653	21.80	9480189	3.77	-1.68	-3.38	fop_j
22000654	19.28	9527334	9.91	9.61	2.43	wolfgang_h
22000655	16.21	9527915	9.89	3.72	-9.17	wolfgang_h
22000656	20.28	9527915	7.87	-6.97	-3.65	wolfgang_h
22000657	20.83	9527915	7.17	-1.75	6.96	wolfgang_h
22000658	21.30	9527915	4.66	4.61	-0.68	wolfgang_h
22000659	15.98	9529744	3.43	-3.22	-1.19	fop_k
22000660	18.80	9532637	3.68	-3.39	-1.43	fop_i
22000661	16.92	9533489	1.13	-1.13	0.07	fop_k roboAO_LP600
22000662	21.20	9534832	1.86	-1.53	-1.05	fop_k
22000663	17.05	9574179	0.34	-0.25	0.23	fop_k
22000664	20.54	9579641	2.43	1.59	-1.84	fop_k
22000665	16.39	9591728	0.60	0.18	-0.57	roboAO_LP600
22000666	18.15	9592850	1.31	0.23	-1.29	fop_j
22000667	20.86	9594184	3.65	3.12	1.91	fop_j
22000668	20.38	9597411	3.96	1.75	-3.56	fop_j
22000669	14.43	9634821	9.79	-3.03	9.31	wolfgang_jhk
22000670	14.55	9635520	1.04	0.70	0.77	roboAO_LP600
22000671	20.54	9640931	3.87	2.58	2.88	fop_j
22000672	14.97	9640976	0.47	0.06	-0.47	fop_i roboAO_i
22000673	13.00	9662475	2.54	2.50	0.40	fop_j
22000674	19.53	9664276	1.24	0.56	-1.10	roboAO_LP600
22000675	16.45	9697131	1.63	0.45	-1.56	dressing fop_k
22000676	17.81	9702072	8.11	2.31	-7.77	wolfgang_h

ID	Kp	hostID	sep	ΔRA	ΔDec	source
22000677	17.71	9702072	9.45	4.91	8.07	wolfgang_h
22000678	20.54	9705459	3.73	-3.40	1.52	fop_j
22000679	25.84	9710326	3.42	-2.44	-2.40	fop_gri
22000680	24.53	9710326	3.84	-1.49	-3.54	fop_gri
22000681	23.70	9710326	3.86	3.06	-2.36	fop_gri
22000682	14.81	9716028	0.18	-0.02	0.18	fop_692
22000683	19.29	9717943	3.50	-2.87	2.00	fop_j
22000684	17.74	9718066	2.85	0.59	2.79	fop_j
22000685	20.98	9761882	3.53	2.95	-1.95	fop_j
22000686	20.97	9762514	3.23	3.17	-0.59	fop_j
22000687	20.31	9776907	1.89	-0.83	-1.70	fop_k
22000688	17.57	9777090	2.18	0.38	2.15	fop_j
22000689	14.74	9821428	0.11	-0.11	0.02	fop_jk
22000690	16.77	9834731	1.14	1.06	0.43	roboAO_LP600
22000691	17.23	9837083	1.28	1.26	0.24	fop_j
22000692	18.30	9838582	0.13	0.11	0.07	fop_k
22000693	20.30	9843517	2.90	-1.13	2.66	fop_j
22000694	16.70	9843517	0.40	-0.20	-0.35	roboAO_LP600
22000695	12.73	9872292	0.13	0.04	-0.12	fop_k
22000696	15.60	9880467	3.52	-3.52	-0.11	fop_gri roboAO_LP600
22000697	21.60	9886361	7.70	7.51	-1.71	dressing
22000698	20.90	9886361	9.85	4.05	-8.97	dressing
22000699	17.82	9886661	9.91	-9.51	2.80	wolfgang_h
22000700	16.04	9895006	0.87	-0.71	0.50	roboAO_LP600
22000701	19.20	9896435	3.90	1.96	-3.37	fop_j
22000702	20.62	9899233	3.48	3.46	0.32	fop_j
22000703	20.58	9899233	3.58	2.63	-2.43	fop_j
22000704	16.18	9935983	0.85	-0.70	0.48	fop_jk
22000705	10.74	9941662	1.15	-1.14	0.19	fop_692 roboAO_i
22000706	18.30	9963524	9.05	8.79	2.14	dressing
22000707	17.75	9964801	1.89	-0.49	-1.82	fop_i
22000708	15.28	9966219	0.65	0.65	-0.05	roboAO_LP600
22000709	15.55	9967884	0.53	-0.13	0.51	roboAO_LP600
22000710	12.16	10002261	0.71	0.61	-0.36	fop_jk
22000711	21.29	10004738	2.27	2.08	0.93	fop_gri
22000712	24.04	10004738	2.67	2.48	-1.00	fop_gri
22000713	18.69	10027247	0.11	0.01	0.11	fop_692
22000714	20.40	10027247	3.89	-1.95	3.36	fop_j
22000715	18.09	10028352	2.27	2.25	0.27	wolfgang_k wolfgang_k
22000716	13.03	10057494	0.06	0.05	-0.04	fop_692

ID	Kp	hostID	sep	ΔRA	ΔDec	source
22000717	21.32	10073672	3.98	3.97	0.32	fop_j
22000718	16.28	10090854	0.23	0.23	-0.02	roboAO_LP600
22000719	16.55	10122538	0.33	0.09	0.32	roboAO_LP600
22000720	18.24	10136549	1.35	0.40	-1.29	fop_k
22000721	20.74	10157573	3.42	1.72	2.95	fop_j
22000722	14.42	10158418	0.30	-0.28	0.09	fop_jk roboAO_LP600 wolfgang_k
22000723	19.94	10190777	2.38	-2.14	-1.05	wolfgang_h
22000724	12.71	10191056	1.32	-0.54	1.21	roboAO_LP600
22000725	16.00	10206675	0.91	0.33	0.85	fop_h roboAO_LP600
22000726	20.75	10206675	2.55	1.72	1.88	fop_h
22000727	20.23	10213902	3.06	3.06	0.12	fop_j
22000728	19.70	10221505	1.30	0.47	-1.21	roboAO_LP600
22000729	12.42	10264660	0.25	0.15	-0.20	adams_A adams_P fop_692 roboAO_i
22000730	19.90	10264660	5.60	4.25	3.65	adams_A
22000731	19.50	10264660	5.27	4.27	3.09	adams_P
22000732	20.77	10275805	3.98	-3.80	1.18	fop_j
22000733	14.30	10287248	0.59	0.02	0.59	fop_LP600 roboAO_LP600
22000734	19.31	10287723	0.65	-0.53	-0.38	fop_jk
22000735	18.25	10332883	1.70	1.68	-0.26	fop_LP600 roboAO_LP600 wolfgang_k
22000736	23.90	10340423	2.63	2.26	-1.34	fop_gri
22000737	18.07	10353968	8.36	-5.03	-6.67	wolfgang_k
22000738	20.69	10360722	1.51	-1.26	0.83	fop_k
22000739	20.57	10395543	8.05	1.44	-7.92	wolfgang_h
22000740	15.97	10397751	0.47	-0.46	0.10	roboAO_LP600
22000741	18.15	10454313	0.97	-0.76	-0.60	roboAO_LP600
22000742	20.81	10454632	3.53	1.66	-3.12	wolfgang_h
22000743	13.74	10470206	1.86	1.65	-0.85	fop_j
22000744	20.73	10471515	1.95	-1.93	-0.32	dressing fop_k
22000745	15.81	10471621	0.35	0.17	-0.30	roboAO_LP600
22000746	20.20	10489525	2.07	-1.95	-0.68	adams_P
22000747	20.70	10489525	5.28	3.21	-4.19	adams_P
22000748	20.60	10489525	5.53	4.27	-3.52	adams_P
22000749	22.09	10489525	3.85	-2.43	-2.99	fop_j
22000750	11.76	10514429	3.28	-3.28	-0.06	fop_j
22000751	11.30	10514430	3.19	3.19	-0.08	adams_A adams_P
22000752	19.75	10531955	2.80	2.66	-0.86	fop_h
22000753	13.34	10547685	2.73	2.07	1.79	fop_j
22000754	14.54	10548411	2.73	-0.15	-2.73	fop_j
22000755	20.79	10583066	3.91	0.24	-3.90	fop_j wolfgang_h

ID	Kp	hostID	sep	ΔRA	ΔDec	source
22000756	22.09	10583066	9.22	-8.97	2.15	wolfgang_h
22000757	19.94	10583180	3.63	2.95	2.11	fop_j
22000758	17.70	10593626	5.37	0.24	-5.36	adams_P
22000759	20.10	10593626	5.40	5.22	1.38	adams_P
22000760	17.23	10597693	1.15	-0.98	0.61	roboAO_LP600
22000761	18.08	10604335	0.73	-0.60	-0.42	fop_k
22000762	16.52	10604521	0.35	-0.23	-0.26	roboAO_LP600
22000763	17.91	10621666	2.99	-0.74	2.90	fop_deltaKp=DeltaV
22000764	18.94	10647452	2.46	-2.06	1.34	roboAO_LP600
22000765	20.55	10676750	3.70	3.01	-2.14	fop_j
22000766	19.21	10684670	1.51	1.42	-0.52	roboAO_LP600
22000767	12.89	10685764	0.41	-0.15	-0.39	fop_692
22000768	17.47	10779233	0.96	0.63	0.73	fop_692 roboAO_LP600
22000769	18.88	10794087	2.86	2.80	-0.61	adams_C fop_k fop_k
22000770	17.02	10810838	0.55	0.53	0.15	adams_C fop_LP600 roboAO_LP600
22000771	17.78	10864656	0.88	0.32	0.82	fop_j
22000772	17.25	10873260	6.62	0.84	-6.56	wolfgang_k
22000773	14.83	10875007	1.69	1.52	0.74	fop_j roboAO_LP600
22000774	14.99	10905911	0.78	-0.77	-0.13	dressing fop_692 roboAO_LP600
22000775	18.31	10928043	1.73	0.77	1.56	fop_j wolfgang_k
22000776	12.22	10967168	1.65	0.81	1.44	fop_j
22000777	15.37	10975146	0.75	-0.04	0.74	fop_h roboAO_LP600
22000778	13.97	10984090	0.11	0.10	-0.05	adams_P fop_692
22000779	15.68	11030475	0.15	-0.00	0.15	fop_gri
22000780	21.58	11030475	6.43	5.87	2.61	wolfgang_h
22000781	19.32	11030475	8.38	1.67	-8.21	wolfgang_jhk wolfgang_hk
22000782	16.65	11037511	0.60	0.26	-0.54	roboAO_LP600
22000783	13.36	11075429	0.31	0.12	0.29	roboAO_LP600
22000784	15.72	11075737	0.37	0.32	-0.20	adams_P fop_jk
22000785	12.68	11081504	0.60	0.58	0.13	fop_692 roboAO_LP600
22000786	20.20	11086270	2.40	-1.58	1.80	adams_P
22000787	18.72	11100383	1.51	-0.22	1.49	wolfgang_h
22000788	20.90	11100383	7.29	6.26	3.73	wolfgang_h
22000789	21.51	11100383	7.10	2.18	6.76	wolfgang_h
22000790	15.54	11181260	0.77	-0.45	0.62	roboAO_LP600
22000791	18.46	11187436	2.88	0.60	-2.82	roboAO_LP600
22000792	14.33	11192141	0.34	-0.06	0.33	fop_692
22000793	20.26	11193263	3.09	-1.71	-2.58	fop_h
22000794	14.83	11197853	1.06	-1.05	-0.15	dressing fop_k roboAO_LP600

ID	Kp	hostID	sep	ΔRA	ΔDec	source
22000795	12.93	11231334	1.16	1.12	0.32	adams_A adams_A fop_692 fop_jk roboAO_i
22000796	18.57	11236244	2.32	-0.57	-2.25	fop_j roboAO_LP600
22000797	15.74	11246364	0.06	0.05	0.03	fop_k
22000798	21.72	11246364	1.29	1.04	0.76	fop_k
22000799	14.85	11253711	1.05	-0.96	-0.43	roboAO_LP600
22000800	18.62	11253827	0.63	-0.50	0.39	fop_692
22000801	17.59	11259686	1.60	-1.50	-0.55	fop_jk
22000802	15.76	11297236	0.16	0.03	0.16	fop_692
22000803	23.17	11305996	0.80	0.05	-0.80	fop_gri
22000804	20.38	11342573	3.65	2.30	2.83	fop_j
22000805	20.86	11351454	3.43	-1.73	-2.97	fop_j
22000806	16.85	11351454	0.77	-0.70	-0.31	roboAO_LP600
22000807	14.69	11358389	0.77	-0.71	-0.29	roboAO_LP600
22000808	17.99	11360571	1.12	1.07	-0.35	roboAO_LP600
22000809	13.33	11401253	1.40	0.64	-1.25	roboAO_LP600
22000810	16.67	11401822	1.57	-0.64	1.43	fop_j
22000811	17.60	11403339	2.16	-1.47	1.58	fop_LP600 roboAO_LP600
22000812	15.57	11403389	0.31	-0.16	-0.26	roboAO_LP600
22000813	15.51	11446443	1.12	0.78	-0.80	fop_692 roboAO_i
22000814	16.43	11453592	1.89	-1.58	1.03	fop_h roboAO_LP600 wolfgang_jk
22000815	21.13	11453592	5.98	-5.59	2.14	wolfgang_j
22000816	19.53	11456382	4.49	4.38	0.98	wolfgang_h
22000817	20.38	11456382	8.01	5.77	-5.55	wolfgang_h
22000818	16.15	11460018	6.94	-2.75	6.37	wolfgang_k
22000819	18.00	11460018	8.49	-3.84	-7.57	wolfgang_k
22000820	19.23	11460018	1.19	0.29	-1.15	wolfgang_k
22000821	14.78	11462341	0.06	0.05	0.04	fop_LP562
22000822	12.96	11462556	0.87	-0.85	-0.15	fop_jk roboAO_LP600
22000823	15.96	11465813	1.77	-1.74	0.36	fop_jk roboAO_LP600
22000824	17.86	11497958	0.22	-0.13	-0.17	fop_gri
22000825	15.70	11499192	1.14	-1.13	0.16	roboAO_LP600
22000826	17.89	11551652	3.29	2.60	2.02	fop_jk
22000827	13.64	11565924	0.35	0.24	-0.26	fop_692 roboAO_LP600
22000828	17.51	11566064	1.04	0.41	0.96	fop_k
22000829	18.56	11566064	1.43	-1.19	-0.79	fop_k
22000830	17.13	11600889	2.18	2.06	0.74	fop_j roboAO_i wolfgang_hk
22000831	22.68	11601584	1.93	-1.42	1.30	fop_gri
22000832	20.95	11601584	2.23	0.68	2.13	fop_gri
22000833	21.87	11601584	2.75	2.73	0.34	fop_gri

ID	Kp	hostID	sep	ΔRA	ΔDec	source
22000834	21.48	11611600	2.82	2.42	1.44	fop_j
22000835	16.55	11621223	6.58	-3.74	5.42	wolfgang_h
22000836	20.26	11621223	4.65	-3.84	2.62	wolfgang_h
22000837	16.73	11624249	0.56	-0.34	-0.44	fop_LP600 roboAO_LP600
22000838	16.39	11671579	0.11	0.01	-0.11	fop_k
22000839	14.69	11671646	1.48	-1.26	0.76	fop_jk
22000840	15.74	11701407	0.40	-0.22	-0.34	roboAO_LP600
22000841	14.39	11764462	0.40	0.40	-0.06	fop_692 roboAO_LP600
22000842	17.38	11768142	0.18	-0.06	-0.17	fop_gri fop_gri
22000843	22.20	11804465	5.04	3.27	-3.84	adams_P
22000844	17.56	11853130	0.81	-0.81	0.08	fop_k roboAO_LP600
22000845	17.74	11858979	1.49	0.70	1.32	roboAO_LP600
22000846	13.57	11869052	1.53	1.19	-0.97	fop_j
22000847	17.48	11874577	0.98	0.86	0.48	roboAO_LP600
22000848	16.70	11875511	0.58	-0.42	-0.40	fop_692 roboAO_LP600
22000849	19.93	11913013	3.49	-3.02	1.74	fop_deltaKp=DeltaJ
22000850	13.73	11967788	1.83	1.68	-0.73	fop_jk roboAO_LP600
22000851	18.30	12009917	0.69	-0.68	-0.15	fop_jk
22000852	16.04	12069414	0.39	-0.21	0.33	fop_i
22000853	14.88	12105051	1.08	0.24	1.05	adams_A fop_jk roboAO_i
22000854	20.40	12121570	0.34	-0.22	-0.26	fop_gri
22000855	12.51	12167361	0.93	0.50	0.78	fop_692
22000856	18.91	12168895	2.80	-0.45	-2.76	fop_k
22000857	16.22	12204137	0.87	-0.30	0.82	roboAO_LP600
22000858	22.30	12252424	5.14	-5.12	0.47	adams_P
22000859	18.12	12254792	1.15	0.28	1.12	roboAO_LP600
22000860	20.69	12256520	0.95	0.92	-0.23	fop_gri
22000861	23.92	12256520	3.39	0.69	-3.32	fop_gri
22000862	13.96	12301181	0.38	-0.36	0.13	fop_692 roboAO_LP600
22000863	15.23	12314973	0.92	-0.84	-0.36	fop_692
22000864	18.57	12356617	3.19	-2.60	1.85	fop_k
22000865	16.43	12400538	0.77	0.74	-0.23	roboAO_i
22000866	17.55	12404305	3.45	3.30	1.02	fop_j
22000867	16.89	12404954	8.57	8.28	-2.19	wolfgang_k
22000868	20.40	12416661	4.44	3.67	2.49	dressing
22000869	14.49	12418418	0.04	0.03	-0.03	fop_deltaKp=Delta880
22000870	13.74	12454461	0.61	0.50	-0.36	fop_h roboAO_i
22000871	16.71	12456063	1.89	1.67	-0.88	fop_jk roboAO_LP600
22000872	23.42	12470844	2.73	2.71	-0.34	fop_gri
22000873	13.11	12785320	2.05	-2.05	0.05	fop_jk roboAO_LP600

ID	Kp	hostID	sep	ΔRA	ΔDec	source
22000874	16.80	12785320	2.01	2.01	-0.11	fop_i

References

Adams, E., et al. 2012, AJ, 144, 2

Baranec, C., et al. 2016, ApJ 152, 1

Brown, T. M., et al. 2011, ApJ 142, 112

Bryson, S. T., et al. 2010a, ApJ 713, L97

Bryson, S. T., et al. 2010b, Proc. SPIE 7740, 77401D

Bryson, S. T., et al. 2013, PASP 125, 889

Bryson, S., et al. 2016, *The Kepler Certified False Positive Table*, KSCI-19093-002

Burke, C. J., et al. 2014, ApJS 210, 19

Coughlin, J., et al. 2014, ApJ 147, 119

Coughlin, J., et al. 2016, ApJS 224, 12

Dressing, C., et al. 2014, AJ, 148, 5

Efron, B. and Tibshirani, R. J. 1994, *An Introduction to the Bootstrap*, CRC Press

Furlan, E., et al. 2016, AJ, *in press* (arxiv:1612.02392)

Gregory, P. 2010, *Bayesian Logical Data Analysis for the Physical Sciences*, Cambridge University Press

Howell, S., et al. 2012, ApJ 746, 2

Jenkins, J., et al. 2010, Proc. SPIE 7740, 77400D

Jenkins, J., et al. 2017, *Kepler Data Processing Handbook*, KSCI-19081-002

Koch, D., et al. 2010, ApJ 713, L79

Law, N. M., et al. 2014, ApJ 791, 1

Lawrence, A., et al. 2007, MNRAS 379, 1599

Levenberg, K. 1944, Quarterly of Applied Mathematics 2, 164

Marquardt, D. W. 1963, Journal of the Society for Industrial and Applied Mathematics, 11, 431

Morton, T. D., and Johnson, J. A. 2011, ApJ 738, 170

Mullally, F., et al. 2015, ApJS 217, 31

Scott, D. W. 1992, *Density Estimation: Theory, Practice and Visualization*, John Wiley & Sons, New York, Chichester

Silverman, B. W. 1986, *Density Estimation for Statistics and Data Analysis*, Chapman & Hall, London

Thompson, S., et al. 2017, *in prep.*

Van Cleve, J., et al. 2016, *Kepler Data Characteristics Handbook*, KSCI-19040-005

Wolfgang, A., 2015, *Leveraging the Power of a Planet Population*, UC Santa Cruz: Astronomy & Astrophysics. Retrieved from: http://escholarship.org/uc/item/08k2g3tb

Ziegler, C., et al. 2016, Proc. SPIE 9909, 99095U